AD_____

Award Number: DAMD17-02-1-0361

TITLE: Cancer Immunology in an Inducible Model of Breast Cancer

PRINCIPAL INVESTIGATOR: Khashayarsha Khazaie, Ph.D.

CONTRACTING ORGANIZATION: Dana-Farber Cancer Institute
Boston, MA 02115

REPORT DATE: April 2005

TYPE OF REPORT: Final

PREPARED FOR: U.S. Army Medical Research and Materiel Command
Fort Detrick, Maryland 21702-5012

REPORT DOCUMENTATION PAGE

Form Approved
OMB No. 074-0188

1. AGENCY USE ONLY (Leave blank)	2. REPORT DATE	3. REPORT TYPE AND DATES COVERED
	April 2005	Final (1 Apr 2002 - 31 Mar 2005)

4. TITLE AND SUBTITLE
Cancer Immunology in an Inducible Model of Breast Cancer

5. FUNDING NUMBERS
DAMD17-02-1-0361

6. AUTHOR(S)
Khashayarsha Khazaie, Ph.D.

7. PERFORMING ORGANIZATION NAME(S) AND ADDRESS(ES)
Dana-Farber Cancer Institute
Boston, MA 02115

E-Mail: Khashayarsha_khazaie@dfci.harvard.edu

8. PERFORMING ORGANIZATION REPORT NUMBER

9. SPONSORING / MONITORING AGENCY NAME(S) AND ADDRESS(ES)
U.S. Army Medical Research and Materiel Command
Fort Detrick, Maryland 21702-5012

10. SPONSORING / MONITORING AGENCY REPORT NUMBER

11. SUPPLEMENTARY NOTES
Original contains color plates: All DTIC reproductions will be in black and white.

12a. DISTRIBUTION / AVAILABILITY STATEMENT
Approved for Public Release; Distribution Unlimited

12b. DISTRIBUTION CODE

13. Abstract (*Maximum 200 Words*) (*abstract should contain no proprietary or confidential information*) Cancer patients can harbor significant numbers of CD8 and CD4 T cells with specificities to tumor Ags. Yet, in most cases, such T cells fail to eradicate the tumor *in vivo*, reflecting the partial or total compromise of tumor specific immune surveillance In the course of the past year we investigated the interference of Ag-specific $CD4^{+}CD25^{+}$ regulatory T (Treg) cells with the tumor-specific CD8 T cell immune response *in vivo*, by monitoring the homing, expansion and effector function of both subsets in draining and non-draining lymph nodes. The results show that CD8 cells expand to the same extent and produce similar levels of IFN-γ in the presence or absence of Ag-specific Treg. Intravital imaging studies have revealed normal interaction of the cytotoxic T cells with HA expressing target cells within tumor draining lymph nodes, as well as release of granules by the T cells, but absence of any killing activity. Thus, Tregs abrogate CD8 T cell-mediated tumor rejection by specifically suppressing the cytotoxicity of expanded CD8 cells. The molecular mechanism of suppression involves TGF-β since expression of a dominant negative TGF-β receptor by tumor-specific CD8 cells renders them resistant to suppression and is associated with tumor rejection and unimpaired cytotoxicity, highlight the potential therapeutic sense of targeting TGF-β receptor signaling, for enhancing anti tumor T cell responses.

14. SUBJECT TERMS
Whey Acidic Protein, Cre/loxP, b-catenin, mammary-tumor, tumor-antigen, T cell receptor transgenic mice, T cell/bone marrow reconstitution, tolerance, immune reactivity, therapy

15. NUMBER OF PAGES
37

16. PRICE CODE

17. SECURITY CLASSIFICATION OF REPORT	18. SECURITY CLASSIFICATION OF THIS PAGE	19. SECURITY CLASSIFICATION OF ABSTRACT	20. LIMITATION OF ABSTRACT
Unclassified	Unclassified	Unclassified	Unlimited

Table of Contents

INTRODUCTION: Narrative that briefly (one paragraph) describes the subject, purpose and scope of the research.

The growth of mammary tumors reflects the failure of antitumor T cell responses. This is likely to have both systemic and local causes. Spurious expression of tumor antigens in the thymus could lead to the generation of regulatory T cells, which in turn may suppress specific cytolytic T cells responses. At the site of the tumor, local tissue and tumor microenvironment could also influence tumor-T cell interactions and outcome. By following the function and fate of T cells that recognize a defined antigen, it is possible to define the mechanisms involved in immune evasion by the tumor, and to open possibilities for targeted therapy. In the previous annual reports we described animal model of autochtonous mammary cancer. It was also reported that transgenic expression of an ectopic antigen (influenza hemagglutinin: HA) led to the generation of HA specific regulatory T cells, and that this was directly linked to the spurious intrathymic expression of this antigen. Over the course of the past year, we have made progress in understanding in detail the impact of the presence of physiological levels of tumor specific regulatory T cells on anti-tumor cytolytic T cell responses. Furthermore, we have gained insight into the mechanisms of immune suppression and signaling pathways involved in rendering antigen specific cytotoxic CD8+ T cells incapable of rejecting the tumor.

BODY: This section of the report shall describe the research accomplishments associated with each task outlined in the **approved** Statement Of Work.

Tregs suppress antigen specific CD8 T-cell mediated cytotoxicity.

In the recent years it has become increasingly clear that systemic immune tolerance plays a major role in preventing autoimmunity. In the context of cancer, systemic tolerance to tumor antigens is a key factor in hindering tumor rejection. A common denominator is the promiscuous expression of tissue and/or tumor specific genes in the thymus. Recent observations in transgenic mice suggest promiscuous expression in the thymus of particular tumor antigens (1). One consequence of this may be the intrathymic generation of regulatory T cells that suppress immune responses against tissue/tumor specific antigens (2); for reviews see (3-5). Indeed, adoptive T cell transfer together with myeloablative treatment have provided promising results in the treatment of melanoma patients (6), supporting the view that depletion of regulatory cells prior to immunotherapy can be beneficial, in controlling cancer.

Our observations, summarized in the last two yearly reports, indicate that transgenic expression of the influenza coat protein (hemaglutinin: HA) leads to the generation of antigen specific regulatory T cells that migrate from the thymus and are maintained in the peripheral lymphatics. To reveal the impact of T cell regulation on the host anti-HA immune response, we performed series of experiments that relied on the adoptive transfer of HA specific regulatory T cells. Tumors expressing or not expressing HA grew equally well in transplanted mice, revealing the lack of an efficient tumor-specific immune response against HA. Transfer of HA specific CD8 T cells shortly before tumor challenge resulted in specific rejection of HA expressing tumors. Rejection of CT44 tumors occurred faster when HA–specific CD8 T cells were transferred together with HA–specific CD4 helper T cells (2)). In marked contrast, however, when HA–specific CD8 T cells were transferred together with HA–specific TCR transgenic $CD4^+$ $CD25^+$ T cells (Treg) (2)), CD8 T cell–mediated rejection of HA^+ tumors was abolished. The steady state levels of adoptively transferred T cells in these experiments in the absence of Ag challenge were near physiological, and comparable for both CD4 and CD8 cells, in the range of 0.01% Ag–specific T cells amongst total CD8 or CD4 cells, respectively. These experiments therefore indicate that Treg were able to effectively interfere at early stages with the CD8 immune response.

Aspects of CD8 T cell mediated response not affected by Treg.

Since CD4 Treg were reported to impair CD8 T cell proliferation *in vitro* (7), we investigated whether a similar mechanism contributed to the Treg–dependent impairment of the CD8 immune response *in vivo*. Thus, CFSE–labeled HA–specific Thy1.2 CD8 cells were adoptively transferred into Thy1.1 BALB/c mice that were subsequently challenged with tumors. The number of HA–specific CD8 cells (defined as $Thy1.2^+$ $CD8^+$) rapidly increased 200 fold in the tumor draining LN, accompanied by extensive cell division. Similar accumulation and expansion of HA–specific CD8 cells was observed when co-transferred with HA–specific naïve CD4 cells. The CD4 T cell

population (defined as Thy1.2$^+$ CD4$^+$) also rapidly expanded, reaching 2.9% ± 0.4% of CD4 cells on d 7, which is equivalent to 3.3 ± 2.0 HA–specific CD4 cells per HA–specific CD8 cell. The Ag-specific proliferation of both HA–specific CD8 and CD4 cells in CT44 draining LN indicated that HA peptides were effectively presented in this environment. Since the tumor cells did not express class II MHC molecules the results indicate that HA Ags were released from tumor cells and presented by class II MHC positive cells, most likely dendritic cells, in the draining LN.

In further experiments, the presence of Treg did not alter the expansion of HA–specific CD8 cells as the kinetic of expansion of CD8 cells in the tumor draining LN remained unchanged or only slightly reduced after co-transfer with Treg. This notion was further supported by the observation that the dilution of CFSE label was not significantly different in CD8 cells expanding in the absence or presence of Treg. HA–specific CD4 Treg also accumulated within the same LN, starting from ~0.01% of CD4 cells immediately after adoptive transfer and reaching 3.4% ± 0.8% of all LN CD4 cells on d 7. HA–specific CD4 Treg accumulated faster than HA–specific CD8 cells by d 7. Neither CD8 cells nor Treg accumulated in the LN draining the HA-negative tumor. HA–specific CD4 Treg did not accelerate apoptosis of HA–specific CD8 cells, as the vast majority of cells remained Annexin V–negative in the presence or absence of Treg. Collectively these data indicated that Treg did not interfere with accumulation and division of tumor–specific CD8 cells in the tumor draining LN.

In an attempt to understand the impact of Treg of CD8 T cell differentiation, we analyzed the expression of differentiation cell surface molecules on HA–specific CD8 cells. A significant fraction of Ag–primed HA–specific CD8 cells acquired an activated CD25$^+$ CD127$^-$ CD69$^+$ CD44^{high} CD62L^{low} phenotype, as demonstrated on d 7 in the tumor draining LN (Fig. 1). Similar phenotypic changes were observed when HA–specific CD8 cells were co-transferred with either naive HA–specific CD4 cells or HA–specific CD4 Treg (Fig. 1). Since HA–specific CD8 cells acquired an activated phenotype irrespective of the absence or presence of Treg, expression of these markers were not informative.

The influence of HA–specific Treg on the functional activity of CD8 cells was investigated by analyzing cytokine production in HA–specific CD8 cells on d 7 after tumor challenge. The majority of HA–specific CD8 cells produced IFN-γ and TNF-α upon restimulation with exogenous HA peptide or PMA/Ionomycin. Co-transfer of HA–specific CD4 Treg with HA–specific CD8 cells did not inhibit cytokine production. This was so whether the cells were restimulated only with class I MHC–restricted peptide, both class I and class II MHC–restricted peptides or with PMA and ionomycin indicating that the reactivation of Treg *in vitro* did not suppress cytokine production by activated CD8 cells.

We further biased the experiments to favor close proximity of CD8 T cells and Tregs during antigen re-stimulation *in vitro*. This was done by exposing the explanted T cells to antigen presenting cells, pulsed with HA specific class I and class II peptides, rather than adding the peptide to the culture medium. The presence of HA–specific CD4 Treg did not interfere with cytokine production by CD8 cells even under these condition (Fig. 2). Collectively these experiments indicate that the Treg did not interfere with the ability of CD8 cells to produce IFN-γ at early stages of the immune response.

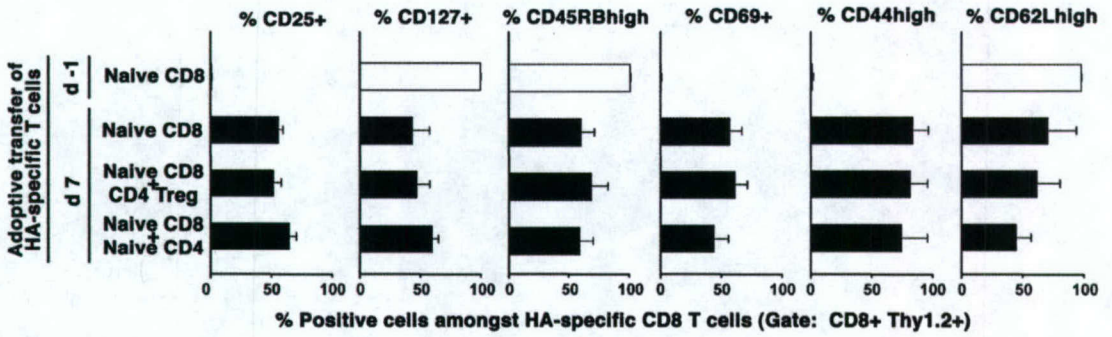

Figure 1 – HA–specific CD4 Treg do not impair the expression of CD8 T cell differentiation markers. Thy1.1 BALB/c mice were adoptively transferred on d –1 with different combinations of Thy1.2 HA–specific T cells and challenged with CT44 (HA^+) tumors on d 0. HA–specific CD8 T cells (defined as $CD8^+$ $Thy1.2^+$) were collected from CT44 draining LN and subjected to phenotypic analysis. Their phenotype was compared with the one displayed by naive HA–specific CD8 T cells that were used for adoptive transfer on d –1. Results show mean and S.D. values of 6 mice from 2 independent experiments.

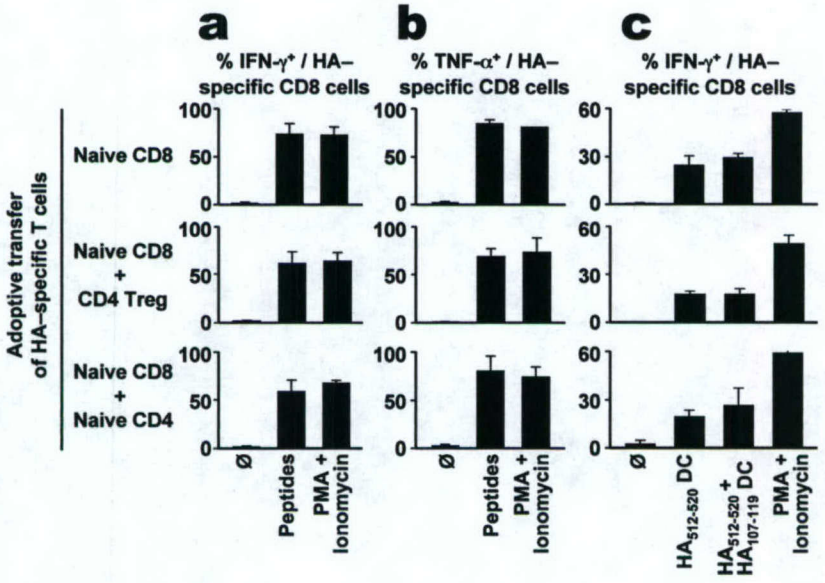

Figure 2 – HA–specific CD4 Treg do not control the production of inflammatory cytokines by HA–specific CD8 T cells. Thy1.1 BALB/c mice were adoptively transferred on d –1 with different combinations of Thy1.2 HA–specific T cells, challenged with (HA^+) tumors on d 0. Tumor draining LN cells were collected on d 6. HA–specific CD8 T cells were analyzed for (a) IFN-γ (b) TNF-α production after 4 h restimulation with exogenously added $HA_{512-520}$ and $HA_{107-119}$ peptides or PMA and Ionomycin. (c) HA–specific CD8 T cells were analyzed for IFN-γ production after 4 h restimulation with DC previously pulsed with only $HA_{512-520}$ or both $HA_{512-520}$ and $HA_{107-119}$ peptides, or PMA and Ionomycin. Results show mean and S.D. values of ≥9 mice from ≥3 independent experiments.

The cytotoxicity of HA–specific CD8 cells was addressed by *in vivo* readouts on day 6 after tumor challenge. In the absence of HA–specific CD4 Treg, HA–specific CD8 T

cells specifically killed $HA_{512-520}$ peptide–pulsed targets in tumor draining LNs. The presence of HA–specific CD4 Treg abolished the specific cytotoxic activity of HA–specific CD8 cells. No *in vivo* killing of HA^+ targets was observed in mice that did not receive HA–specific CD8 cells. Importantly, since Treg did not interfere with the proliferation of naive CD8 cells, the observed reduced cytotoxic activity in the presence of Treg in the tumor draining LNs indicated direct suppression of cytolytic activity rather than indirect suppression through impairment of proliferation.

Mechanism of suppression of tumor specific CD8 T-cell cytotoxicity by Treg.

A potential role of TGF-β in the suppression of tumor rejection by CD8 cells was analyzed by introducing a dominant negative TGF-β receptor into the tumor-specific CD8 cells, by crossing mice with the transgenic TCR specific for $K_d/HA_{512-520}$ with mice harboring a dominant negative TGFbR type II (dnTGFbR) (8). Expression of dnTGFbR by HA–specific CD8 cells did not alter their naïve phenotypic status at least in 4–6 wk old animals, as the vast majority of both dnTGFbR and *wt* HA–specific CD8 cells were $CD25^-$ $CD127^+$ $CD45RB^{high}$ $CD69^-$ $CD44^{low}$ $CD62L^{high}$ (Fig. 3). When 10^5 dnTGFbR or *wt* HA–specific CD8 cells were transferred into BALB/c mice both populations of cells displayed similar kinetics of expansion in response to challenge with CT44 tumors and rejected CT44 tumors. Thus, expression of the dnTGFbR in CD8 cells did not alter their expansion and the kinetic of tumor rejection. When co-injected with Treg, dnTGFbR and *wt* HA–specific CD8 cells also similarly expanded in response to challenge with CT44 tumors. However, expression of dnTGFbR by HA–specific CD8 cells interfered with the suppression of tumor immunity by Treg since the kinetic of tumor rejection mediated by dnTGFbR HA–specific CD8 cells was comparable to the one mediated by *wt* HA–specific CD8 cells in the absence of Treg (Fig. 4). In order to address whether this resulted from a failure of Treg to suppress cytotoxicity, the effector function of dnTGFbR and *wt* CD8 cells in CT44 draining LN on d 7 was compared. While the HA–specific CD8 cells efficiently lysed HA–peptide pulsed syngeneic target cells *in vivo* only in the

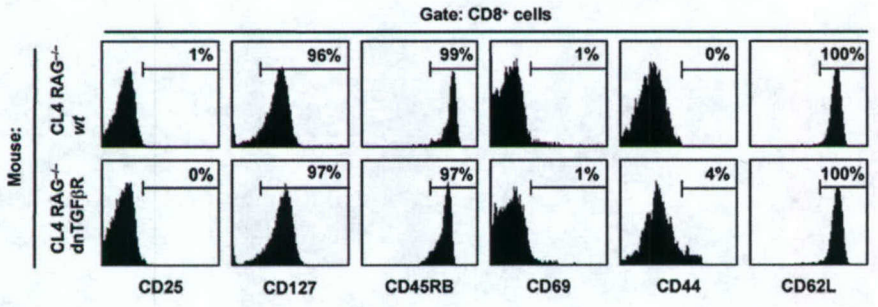

Figure 3. Expression of a dominant negative TGFbR type II does not affect CD8 T cell activation markers. HA–specific CD8 T cells bearing or not a dominant negative TGFbR type II were collected from *TCR-CL4 RAG$^{-/-}$ dnTGFbR* or *TCR-CL4 RAG$^{-/-}$* mice, and were checked for expression of naïve surface markers. Results show mean values of 3 mice.

absence of Treg, the cytotoxicity displayed by dnTGFbR HA–specific CD8 cells in the presence or absence of Treg was indistinguishable (Fig. 4). Thus, expression of

dnTGFbR by HA–specific CD8 cells was sufficient to render CD8 cells resistant to regulation by Treg and allowed efficient tumor rejection by cytolytic activity (9). Furthermore, detailed analysis of HA–specific CD8 T cells showed that HA–specific CD4 Treg did not impair their proliferation. Indeed, 98–99% of the transferred CD8 T cells had homogeneously and extensively divided 6 days after tumor challenge, even in the presence of Treg. Similarly, HA–specific CD4 Treg did not accelerate apoptosis of HA–specific CD8 T cells, as similar numbers of transferred CD8 T cells were stained with Annexin V in the absence or presence of Treg. Similar observations were made 4 days and 8 days after tumor challenge (data not shown) (9). These observations indicate that TGFβ signaling in the CD8 cells is critically required to render them susceptible to Treg mediated regulation. Further experiments were done to understand which aspect of CD8 function was suppressed by the Treg. The observations revealed a novel mechanism for Treg-mediated control of CD8 T cell immune responses.

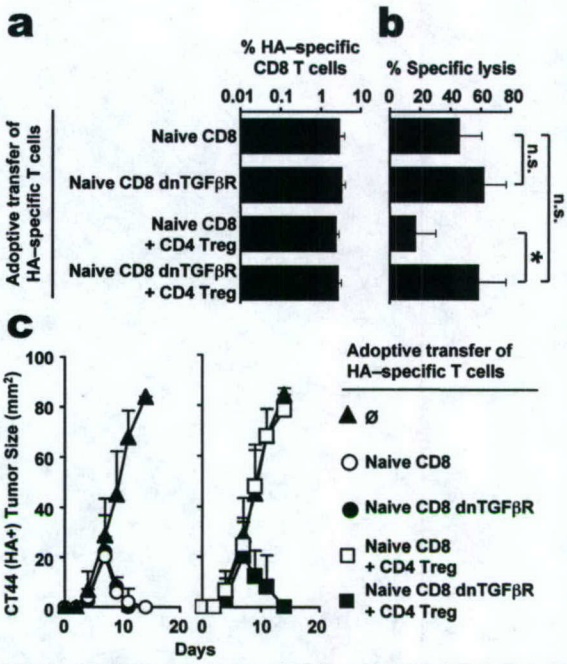

Figure 4. Suppression of HA–specific CD8 T cell cytotoxic activity by HA–specific CD4 Treg requires TGF-b receptor signaling. On d –1, 10^6 naïve HA–specific CD8 T cells expressing or not dnTGFbR were adoptively transferred into BALB/c mice either alone or with 10^5 HA–specific CD4 Treg. Mice were challenged with CT44 (HA^+) tumors on d 0. (a) HA–specific CD8 T cells in CT44 draining LN were quantified on d 6. Mice were injected intravenously with a 1:1 mixture of syngeneic splenocytes previously labeled with 10 μM CFSE and pulsed with $HA_{512-520}$ peptide and of cells previously labeled with 1 μM CFSE but not pulsed with peptide. Tumor draining LN were collected 16 h later and Ag–specific killing of $HA_{512-520}$ positive targets was measured by flow cytometry. (b) *In vivo* cytotoxic activity in CT44 draining LN was measured on d 6. n.s., not significant, *, $p<0.0001$. (c) Tumor size was measured over a period of two weeks, in mice not receiving Treg (left panel) or receiving Treg (right panel). Results show mean and S.D. values of ≥9 mice from ≥3 independent experiments.

In collaboration with the laboratory of Dr. Ullrich von Andrian we embarked on imaging studies of the interaction of cytolytic T cells and their targets with in the tumor draining lymph node, using intravital two photon microscopy. To this aim we first investigated the possibility of using fluorescent dyes to image and distinguish live cells from killed cells. Spleen derived B cells were pulsed with MHC class I HA peptide and labeled with CMTMR and Hoechst 33342. CMTMR is a red fluorescent dye thioether with chloromethyl groups that remains within the cytoplasm and react with thiol groups. Hoechst 33342 is a cell-permeant nuclear dye that emits blue fluorescence when bound to adenine-thymine rich regions of the minor groove of DNA. The labeled cells were then incubated with HA-specific GFP expressing HA specific cytotoxic CD8 T cells *in vitro* in the presence of soluble Annexin V FITC. Confocal fluorescent microscopy revealed that intact cells were negative for Annexin V, and exhibited high red/blue fluorescence ratio intensities, while lysed cells were positive for Annexin V and had low red/blue fluorescence. In apoptotic cells, CMTMR diffused to

the extracellular medium as a consequence of the disruption of membrane integrity, and DNA fragmentation. These preliminary studies validated the usefulness of the dyes, which were then used for *in vivo* studies in anesthetized mice to distinguish intact and lysed cells based on their red/blue fluorescence ratio intensities (Fig. 5).

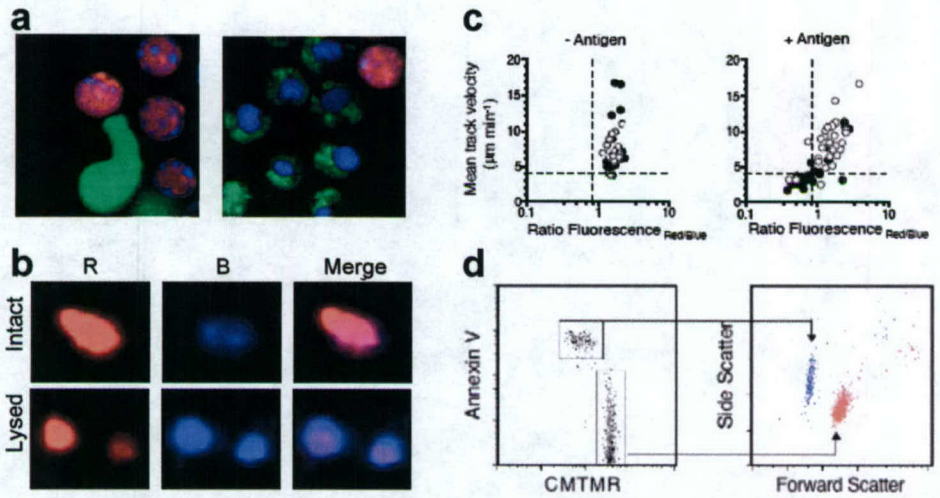

Figure 5. Distinction between intact and lysed cells in vivo. (a) HA+ B cells were labeled with CMTMR and Hoechst 33342, were incubated in vitro with HA-specific GFP+ cytotoxic CD8 T cells in the presence of soluble Annexin V FITC. Intact (left panel) and apoptosing (right panel) target cells, respectively negative or positive for Annexin V, exhibit high and low red/blue fluorescence ratio intensities. Note loss of NCMTMR in lysed cell (right panel), as a consequence of the disruption of membrane integrity, as well as increased concentration of Hoechst 33342 in the nucleus of cells with DNA fragmentation. (b–c) Intravital multiphoton lymph node imaging distinguishes intact and lysed cells based on their red/blue fluorescence ratio intensities (b and c) and mean track velocity (c). (d) Flow cytometry of lymph node cell suspensions confirm a reduction of red fluorescence intensity of lysed (Annexin V+) targets.

To this aim mice were injected with GFP expressing HA specific CD8 T-cells, and transplanted one day later with HA expressing tumor cells. 2-5 days later the mice were injected with HA pulsed splenic B cells that had been labeled with CMTMR and Hoechst 33342, and the tumor draining lymph node was imaged by time-lapse intravital multiphoton microscopy. We found that HA specific CD8 T-cells in tumor draining lymph nodes were highly motile, migrated without apparent directional bias and selectively formed stable conjugates upon encounter with B cell targets that present tumor antigenic peptides. These studies revealed long lasting interactions between the CD8 T cells and their HA+ target cells, which led to the loss of motility of the latter and finally target cell lysis, as monitored by recording their red/blue fluorescence and calculating the corresponding ratio (Fig. 6, a). This mode of imaging allowed us to record *in vivo* the sequences of events that lead to antigen specific cell killing by the CD8 T-cells. Furthermore, it opened the possibility of examining the impact of HA specific Treg on the CD8 T cells.

To investigate the *in vivo* events associated with suppression of CD8 T cell mediated lysis, we repeated the above experiments, however this time co-transferring equal numbers of CD4+CD25+ HA specific Treg together with the CD8 T cells. We then performed intravital multiphoton microscopy and time-lapse recording of the migratory and interactive activities of HA+ target B cells and HA-specific CD8 T cells in the presence of regulatory T cells, in the tumor draining lymph node. Surprisingly, the CD8 T-cells proceeded to make contact with and remained in relatively long term association with their target B cells. However, the long lasting interactions did not result in loss of motility or structural integrity of the target cell (Fig. 6, b-d). These observations indicate that regulatory T cells specifically affect the killing process, presumably by hindering the release or altering the composition of the CD8 T cell derived cytolytic granules. We propose that regulation takes place at the level of T cell priming and leads to a defective

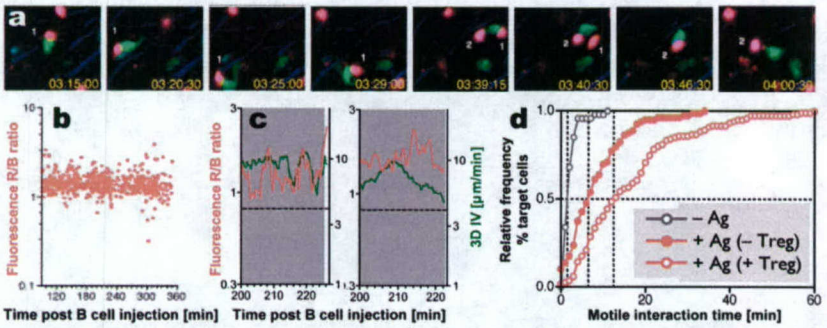

Figure 6. CD4 regulatory T cells control CD8 lysis in vivo. (a) Representative example of time-lapse recording of the migratory and interactive activities of HA+ target B cells (labeled with CMTMR and Hoechst 33342) and HA-specific CD8 T cells (GFP) in the presence of regulatory T cells (not visible here) in tumor draining lymph node and imaged by intravital multiphoton microscopy (b) Absence of target cell lysis at the population level in the presence of regulatory T cells. Each dot represents the red/blue fluorescence ratio of a single target cell at a specific time point (c) Representative examples of the monitoring of red/blue fluorescence ratio, instant velocity and interaction with effector CD8 cells of single target cells over time. Note that long lasting interactions do not result in loss of motility or structural integrity of the target cell. (d) Increased motile interaction time between target cells and CD8 T cells in the presence of regulatory T cells, although killing is not initiated.

differentiation of the disabled effector CD8 T cells. Further experiments are underway to clarify these points.

Tumor–specific CD8 T cells frequently accumulate in metastatic LNs and visceral tumor tissues from cancer patients, but are deficient in mediating cytolytic activity (10). Immunotherapy of patients with cancer requires *in vivo* generation of highly reactive tumor–specific T cells that are not restrained by normal tolerance mechanisms. Lymphodepletion has been recently reported to have a marked effect on the efficacy of adoptive transfer therapy of autologous tumor–specific T cells (6, 11)(our unpublished results; see last report from last year). Here, we propose that the success of this strategy is at least in part related to the pre-activation of the CD8 T cells through lymphopenic expansion. This pre-activation would precede and override the aberrant differentiation of the CD8 T-cells that takes place when naïve T cells are primed in the presence of Treg.

KEY RESEARCH ACCOMPLISHMENTS:

- Using the influenza HA as a model antigen, we have demonstrated that expression of self antigens/tumor antigens results in systemic tolerance to the antigen.
- This systemic tolerance is largely due to the generation of antigen specific CD4+ regulatory T cells (Treg) in the thymus.
- Treg specifically inhibit the killing activity of CD8 T-cells that recognize the same target cells and the Treg.
- The mechanism of inhibition of CD8 T-cell cytolysis is not related to inbition of expansion, migration or even contact of the effector cells with their target cells.
- The mechanism of suppression of CD8 T-cell cytolysis is most likely due to aberrant differentiation of the naïve CD8 T cells in the presence ot Treg, and their failure to produce and/or release cytolytic granules upon contact with target cells.
- Thus, it is no surprise that cancer patients may harbor large numbers of tumor specific T cells that even home to the tumor but are unable to reject their target.
- Overcoming this mode of immune suppression is likely to produce a major breakthrough in the immune therapy of cancer.

REPORTABLE OUTCOMES:

Klein, L., **Khazaie, K.,** von Boehmer, H. 2003 In vivo dynamics of antigen-specific regulatory T cells not predicted from behavior in vitro. **Proc Natl Acad Sci U S A**. 2003 Jul 22;100(15):8886-91.

Psarras, S., Karagianni, N., Kellendonk, C., Tronche, F., Cosset, F. L., Stocking, C., Schirrmacher, V., von Boehmer, H., **Khazaie, K.** 2004 Gene transfer and genetic modification of ES cells by Cre and Cre-PR expressing MESV based retroviral vectors. **Journal of Gene Medicine**. 6: 32-42.

Chen, M.C., Pittet, . J., Weissleder, R., von Boehmer, H., **Khazaie, K.** 2005 Regulatory T cells suppress cytotoxic CD8 T cell function through TGF-b signals *in vivo*. **Proc. Natl Acad. Sci. USA**, 102: (2) 419-424.

Manuscript in preparation:
Pittet, . J.,et al., . 2005 In vivo imaging of the suppression of CD8 T-cells function by Treg. In preparation.

Conclusions

Cancer is likely to outdo the host immune responses at both the systemic and local levels. Immune therapy strategies therefore have to consider strengthening the host at both levels. Action of antigen specific regulatory cells may provide a common mechanism for systemic tolerance, intended to protect against autoimmunity, but also preventing effective immune responses against tumors. Spurious intrathymic expression of self of self antigens as well as the fetal/embryonic class of tumor antigens lead to the generation of potent regulatory T cells. We have demonstrated that *in vivo*, these cells are capable of neutralizing otherwise effective cytolytic activities targeted against the tumor. Understanding the exact mechanism by which regulation works is critical for the design of effective therapeutic intervention. We have shown that immune regulation by Treg is through specific inhibition of the "kiss of death" by the potential cytolytic T cells. Our work has provided an explanation for the presence of relatively high frequencies of tumor specific T cells in cancer patients with progressive disease. Similarly, infiltration of tumors by inactive CD8 T-cells has been demonstrated, and is in agreement with our observations. The first stage of the battle is won, once the tumor specific regulatory cells are eliminated, or the tumor specific cytolytic cells are rendered resistant to regulation. Our work has provided preliminary evidence that the latter is indeed possible to achieve, with relatively simple manipulations of the host prior to adoptive T cell transfer, or possibly vaccination.

REFERENCES:

1. Derbinski, J., A. Schulte, B. Kyewski, and L. Klein. 2001. Promiscuous gene expression in medullary thymic epithelial cells mirrors the peripheral self. *Nat Immunol* 2:1032-1039.
2. Klein, L., K. Khazaie, and H. von Boehmer. 2003. Dynamics of immune regulation in vivo by antigen-specific CD25+CD4+ suppressor T cells. *submitted.*
3. Modigliani, Y., A. Bandeira, and A. Coutinho. 1996. A model for developmentally acquired thymus-dependent tolerance to central and peripheral antigens. *Immunol Rev* 149:155-120.
4. Le Douarin, N., F. Dieterlen-Lievre, and M.A. Teillet. 1996. Quail-chick transplantations. *Methods Cell Biol* 51:23-59.
5. Sakaguchi, S., T. Takahashi, S. Yamazaki, Y. Kuniyasu, M. Itoh, N. Sakaguchi, and J. Shimizu. 2001. Immunologic self tolerance maintained by T-cell-mediated control of self-reactive T cells: implications for autoimmunity and tumor immunity. *Microbes Infect* 3:911-918.
6. Dudley, M.E., J.R. Wunderlich, P.F. Robbins, J.C. Yang, P. Hwu, D.J. Schwartzentruber, S.L. Topalian, R. Sherry, N.P. Restifo, A.M. Hubicki, M.R. Robinson, M. Raffeld, P. Duray, C.A. Seipp, L. Rogers-Freezer, K.E. Morton, S.A. Mavroukakis, D.E. White, and S.A. Rosenberg. 2002. Cancer regression and autoimmunity in patients after clonal repopulation with antitumor lymphocytes. *Science* 298:850-854.
7. Shevach, E.M., R.S. McHugh, C.A. Piccirillo, and A.M. Thornton. 2001. Control of T-cell activation by CD4+ CD25+ suppressor T cells. *Immunol Rev* 182:58-67.
8. Gorelik, L., and R.A. Flavell. 2000. Abrogation of TGFbeta signaling in T cells leads to spontaneous T cell differentiation and autoimmune disease. *Immunity* 12:171-181.
9. Chen, M.L., M.J. Pittet, L. Gorelik, R.A. Flavell, R. Weissleder, H. von Boehmer, and K. Khazaie. 2005. Regulatory T cells suppress tumor-specific CD8 T cell cytotoxicity through TGF-beta signals in vivo. *Proc Natl Acad Sci U S A* 102:419-424.
10. Zippelius, A., P. Batard, V. Rubio-Godoy, G. Bioley, D. Lienard, F. Lejeune, D. Rimoldi, P. Guillaume, N. Meidenbauer, A. Mackensen, N. Rufer, N. Lubenow, D. Speiser, J.C. Cerottini, P. Romero, and M.J. Pittet. 2004. Effector function of human tumor-specific CD8 T cells in melanoma lesions: a state of local functional tolerance. *Cancer Res* 64:2865-2873.
11. Dummer, W., A.G. Niethammer, R. Baccala, B.R. Lawson, N. Wagner, R.A. Reisfeld, and A.N. Theofilopoulos. 2002. T cell homeostatic proliferation elicits effective antitumor autoimmunity. *J Clin Invest* 110:185-192.

Regulatory T cells suppress tumor-specific CD8 T cell cytotoxicity through TGF-β signals *in vivo*

Mei-Ling Chen*†, Mikaël J. Pittet*†‡, Leonid Gorelik§¶, Richard A. Flavell§‖, Ralph Weissleder‡, Harald von Boehmer*,, and Khashayarsha Khazaie*‡***

*Dana–Farber Cancer Institute, Harvard Medical School, Boston, MA 02115; ‡Center for Molecular Imaging Research, Massachusetts General Hospital and Harvard Medical School, Charlestown, MA 02129; and §Section of Immunobiology, School of Medicine, and ‖Howard Hughes Medical Institute, Yale University, New Haven, CT 06520

Communicated by Harvey Cantor, Harvard Medical School, Boston, MA, November 12, 2004 (received for review September 15, 2004)

Cancer patients can harbor significant numbers of CD8 and CD4 T cells with specificities to tumor antigens (Ags). Yet, in most cases, such T cells fail to eradicate the tumor *in vivo*. Here, we investigated the interference of Ag-specific CD4$^+$CD25$^+$ regulatory T cells (Treg) with the tumor-specific CD8 T cell immune response *in vivo*, by monitoring the homing, expansion, and effector function of both subsets in draining and nondraining lymph nodes. The results show that CD8 cells expand to the same extent and produce similar levels of IFN-γ in the presence or absence of Ag-specific Treg. Nevertheless, these Treg abrogate CD8 T cell-mediated tumor rejection by specifically suppressing the cytotoxicity of expanded CD8 cells. The molecular mechanism of suppression involves TGF-β because expression of a dominant-negative TGF-β receptor by tumor-specific CD8 cells renders them resistant to suppression and is associated with tumor rejection and unimpaired cytotoxicity.

CD4$^+$CD25$^+$ regulatory T cells (Treg) are negative regulators of T cell immune responses *in vitro* and *in vivo* (1, 2). Upon TCR ligation, Treg can suppress the proliferation of both CD4 and CD8 cells in coculture experiments (3). Recently, however, it has been shown that the regulation of CD4 T cell responses *in vivo* can have different kinetics (reviewed in ref. 4). When coinjected into normal mice, both Treg and naïve CD4 cells initially proliferate upon recognition of cognate antigen (Ag). Furthermore, Treg do not influence the commitment of Ag-experienced CD4 cells to produce IFN-γ and IL-2. However, Treg do suppress cytokine secretion and interfere with the proliferation and possibly survival of CD4 cells later during the immune response (5–7). Treg also can control the magnitude of recall CD8 T cell responses in different settings that include viral (8, 9) and bacterial (10) infections as well as allograft transplantation *in vivo* (11, 12). A role in Treg function has been attributed to IL-2, which stimulates Treg and in turn may inhibit division of memory CD8 T cells (13, 14). However, these studies did not trace Ag-specific Treg in draining lymph nodes (LN), and it is not clear to what extent the different outcomes reflect accumulation of Treg by specific homing and local expansion. In fact, most studies were conducted with polyclonal Treg of unknown specificity where such questions cannot be addressed, and, therefore, the mode of inhibition cannot be correlated with specific Treg accumulation. Analysis of tumor-bearing patients suggests that suppression of CD8 T cell cytotoxicity by Treg may be causally related to tumor progression, because tumor-specific CD8 cells and tumor-specific CD4 Treg frequently accumulate in tumors from melanoma patients, and tumor-specific CD8 cells fail to exert cytotoxic T lymphocyte effector function (15–17).

This study investigates how Treg suppress primary CD8 T cell immune responses directed against tumor cells expressing influenza hemagglutinin (HA) as a surrogate tumor-specific Ag. Naïve CD8 and regulatory CD4 T cells with transgenic receptors specific for distinct peptides of HA were used to allow us to follow the fate of these cells in tumor draining LN. The results show that Treg interfere with CD8 T cell-mediated tumor rejection relatively early during the immune response, and the mechanism by which Treg suppress naïve CD8 cells differs from the ones that have been reported for memory CD8 cells (10–12, 14). Treg influenced neither the kinetics of proliferation nor the commitment of recently activated CD8 cells to produce inflammatory cytokines. Nevertheless, CD8 cells failed to undergo normal functional maturation in the presence of Treg as evidenced by the fact that their cytotoxic potential to destroy specific targets *in vivo* was abolished. Thus, these experiments reveal a previously unreported fine-tuning by Treg on different effector functions of CD8 cells.

There is considerable controversy over a putative role of TGF-β in the Treg-dependent regulation of immune responses (18). Although two recent studies suggested that TGF-β has a crucial role in the suppression of CD8 T cell-mediated diabetes, perhaps by mechanisms that allow more potent expansion of Treg (19) and mechanisms that may affect unknown functions of CD8 cells (20), the essential role of TGF-β has been debated by others (18). Here, we show that Treg-dependent inhibition of tumor-specific CD8 T cell-mediated cytotoxicity requires expression of the TGF-β receptor by CD8 cells. These data suggest a specific role of TGF-β signaling in the inhibition of cytotoxicity independent of cellular proliferation.

Materials and Methods

Mice. T cell receptor (TCR)-HA recombination activating gene-deficient (RAG$^{-/-}$) mice expressing a TCR specific for *H2-IE*^{d}/HA$_{107-119}$, *TCR-CL4* RAG$^{-/-}$ mice expressing a TCR specific for *H2-K*^{d}/HA$_{512-520}$, and *pgk-HA* $\times$ TCR-HA mice were generated as described in refs. 21, 22, and 23, respectively. BALB/c mice were purchased from Taconic Farms. BALB/c Thy1.1 mice were obtained from Paul Allen (Washington University School of Medicine, St. Louis). Dominant-negative TGFβR type II (dnTGFβRII) B6 mice (24) were backcrossed to *TCR-CL4 RAG*$^{-/-}$ BALB/c mice for five or more generations.

T Cells. HA-specific CD8 cells from *TCR-CL4* RAG$^{-/-}$ mice, HA-specific CD4 cells from *TCR-HA* RAG$^{-/-}$ mice, and HA-specific CD4 Treg from *pgk-HA* $\times$ *TCR-HA* mice were purified as described in ref. 23. Where indicated, cells were labeled with 10 μM carboxyfluorescein diacetate-succinimidyl ester (CFSE; Molecular Probes) prior to adoptive transfer. Dendritic cells (DCs) were magnetically purified (>98% CD11c$^+$) from spleens

Abbreviations: Ag, antigen; CFSE, carboxyfluorescein diacetate-succinimidyl ester; DC, dendritic cell; dnTGFβR, dominant-negative TGFβR type II; HA, influenza hemagglutinin; LN, lymph node; PMA, phorbol 12-myristate 13-acetate; RAG$^{-/-}$, recombination activating gene-deficient; TCR, T cell receptor; Treg, CD4$^+$CD25$^+$ regulatory T cells.

†M.-L.C. and M.J.P. contributed equally to this work.

¶Present address: Biogen Idec, Cambridge, MA 02142.

**To whom correspondence may be addressed at: Dana–Farber Cancer Institute, Harvard Medical School, 44 Binney Street, Smith 736, Boston, MA 02115. E-mail: khashayarsha_khazaie@dfci.harvard.edu or harald_von_boehmer@dfci.harvard.edu.

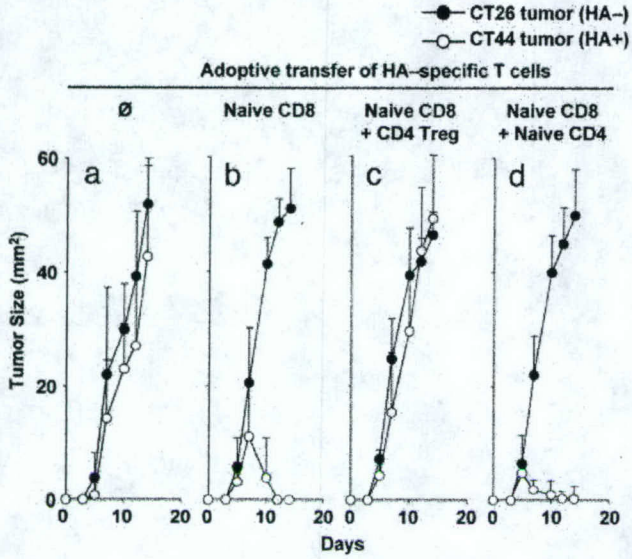

Fig. 1. HA-specific CD8 T cells selectively reject HA-expressing tumors in the absence of HA-specific CD4 Treg. On day −1, BALB/c mice were not treated (*a*) or were adoptively transferred with different combinations of HA-specific T cells as follows: 10^5 naïve CD8 T cells (*b*), 10^5 naïve CD8 T cells and 10^5 CD4 Treg (*c*), or 10^5 naïve CD8 and 10^5 naïve CD4 T cells (*d*). On day 0, two colon carcinoma cell lines, namely CT26 (HA^-) and CT44 (HA^+), were s.c. inoculated in the right and left footpads, respectively. Tumor size was measured over a period of 2 wk. Results show mean and SD values of nine or more mice from at least three independent experiments.

of BALB/c mice that had been implanted with a Flt-3L secreting melanoma cell line (25).

Tumors. The CT26 tumor cell line was derived from a chemically induced murine colon carcinoma. The tumor cell line CT44 was generated by transfecting CT26 cells with a fusion protein of influenza HA and EGFP (23). We injected 10^6 CT44 and CT26 cells s.c. into the upper side of the left and right hind paws of anesthetized animals, respectively (23).

Flow Cytometry. All mAbs were obtained from Becton Dickinson, except anti-HA (clone 37.38), which was obtained from Southern Biotechnology Associates. Anti-TCR-HA (clone 6.5) was purified in our laboratory. Surface and intracellular staining and flow-cytometric analysis were performed as described in ref. 26.

***In Vivo* Cytotoxic T Lymphocyte Assays.** Splenocytes from BALB/c mice were labeled with either 1 or 10 μM CFSE (namely, $CFSE^+$ or $CFSE^{2+}$), then incubated for 1 h at 37°C with either no peptide or 1 μg/ml $HA_{107-119}$ peptide, respectively. Recipient mice were injected i.v. with a 1:1 ratio of the two populations (2×10^7 cells). Tumor-draining LN cells were obtained 16 h later and stained with appropriate mAbs, including anti-B220 mAb. Percentage specific lysis was calculated as follows: % specific lysis = [1 − ($B220^+$ $CFSE^+$ events/$B220^+$ $CFSE^{2+}$ events)] × 100.

Results

Treg Abrogate CD8 Tumor Immunity. The specificity of CD8 T cell-mediated tumor responses was analyzed in normal healthy BALB/c mice that were injected s.c. with both 10^6 HA^+ tumor cells (CT44, right foot) and 10^6 HA^- tumor cells (CT26, left foot) on day 0. Both tumors grew equally well in the transplanted mice, indicating the lack of an efficient tumor-specific immune response in normal mice (Fig. 1*a*). However, adoptive transfer of 10^5 naïve CD8 cells bearing a transgenic TCR specific for the K_d-restricted $HA_{512-520}$ peptide (hereafter termed HA-specific CD8 cells) 1 day before tumor challenge resulted in specific rejection of CT44 tumors (Fig. 1*b*). CD8 T cell-mediated rejection of CT44 tumors was apparent between days 7 and 10 and was complete on day 14 (Fig. 1*b*). In contrast, CT26 tumors within the same individuals were not rejected (Fig. 1*b*).

We then investigated whether CD4 Treg with specificity for a class II-restricted HA epitope may influence primary CD8 T cell immune responses directed against the class I restricted HA peptide (bystander suppression). HA-specific CD4 Treg were obtained from mice expressing influenza-HA under the control of the ubiquitous *pgk* promoter (*pgk-HA*) and a transgenic TCR (*TCR-HA*) specific for the I-E_d-restricted $HA_{107-119}$ peptide (26). BALB/c mice were adoptively transferred with a mixture of 10^5 naïve HA-specific CD8 cells and 10^5 HA-specific CD4 Treg and subsequently challenged with CT26 and CT44 tumors. The results showed that Treg completely abrogated CD8 T cell-mediated rejection of CT44 tumors (Fig. 1*c*), in that the kinetic of CT44 tumor growth was as fast as that displayed by the CT26 tumor within the same individual (Fig. 1*c*), and comparable with the kinetic of CT44 or CT26 tumor growth in mice that did not receive HA-specific CD8 cells (Fig. 1*a*).

In contrast to the Treg-dependent abrogation of CD8 T cell-mediated tumor rejection, the cotransfer of 10^5 nonregulatory CD4 cells with the same specificity as the Treg did not abrogate but rather enhanced tumor rejection by CD8 cells (Fig. 1*d*), in line with the reported role of CD4 cells in augmenting immune responses by CD8 cells (21, 27). As reported in ref. 23, adoptive transfer of naïve HA-specific CD4 cells alone did not mediate rejection of CT44 tumors. The steady-state levels of adoptively transferred T cells in these experiments in the absence of Ag challenge were comparable for both CD4 and CD8 cells, in the range of 0.01% Ag-specific T cells among total CD8 or CD4 cells, respectively. These experiments, therefore, indicate that Treg were able to interfere effectively at early stages with the CD8 immune response.

CD8 T Cell Homing and Expansion. Because CD4 Treg were reported to impair CD8 T cell proliferation *in vitro* (28), we investigated whether a similar mechanism contributed to the Treg-dependent impairment of the CD8 immune response *in vivo*. In initial experiments, CFSE-labeled HA-specific Thy1.2 CD8 cells were adoptively transferred into Thy1.1 BALB/c mice that subsequently were challenged with CT44 and CT26 tumors simultaneously. The number of HA-specific CD8 cells (defined as $Thy1.2^+$ $CD8^+$) rapidly increased 200-fold in CT44 draining LN (Fig. 2 *a* and *b*), whereas HA-specific CD8 cells did not accumulate in CT26 draining LN (Fig. 2*c*). As shown in Fig. 2*b*, the accumulation of CD8 cells in CT44 draining LN was accompanied by extensive cell division. Similar accumulation and expansion of HA-specific CD8 cells was observed when cotransferred with HA-specific naïve CD4 cells (Fig. 2*b*). The CD4 T cell population (defined as $Thy1.2^+$ $CD4^+$) also rapidly expanded in CT44 draining LN, reaching 2.9 ± 0.4% of CD4 cells on day 7, which is equivalent to 3.3 ± 2.0 HA-specific CD4 cells per HA-specific CD8 cell. The Ag-specific proliferation of both HA-specific CD8 and CD4 cells in CT44 draining LN indicated that $HA_{512-520}$ and $HA_{107-119}$ peptides were effectively presented in this environment. Because CT44 tumor cells do not express class II MHC molecules, the results indicate that HA Ags were released from tumor cells and presented by class II MHC positive cells, most likely DCs, in the draining LN.

In further experiments, the fate of HA-specific CD8 cells that were cotransferred with HA-specific CD4 Treg was studied. The presence of Treg did not alter the expansion of HA-specific CD8 cells because the kinetic of expansion of CD8 cells in the CT44 draining LN remained unchanged or only slightly reduced after cotransfer with Treg. This notion was further supported by the

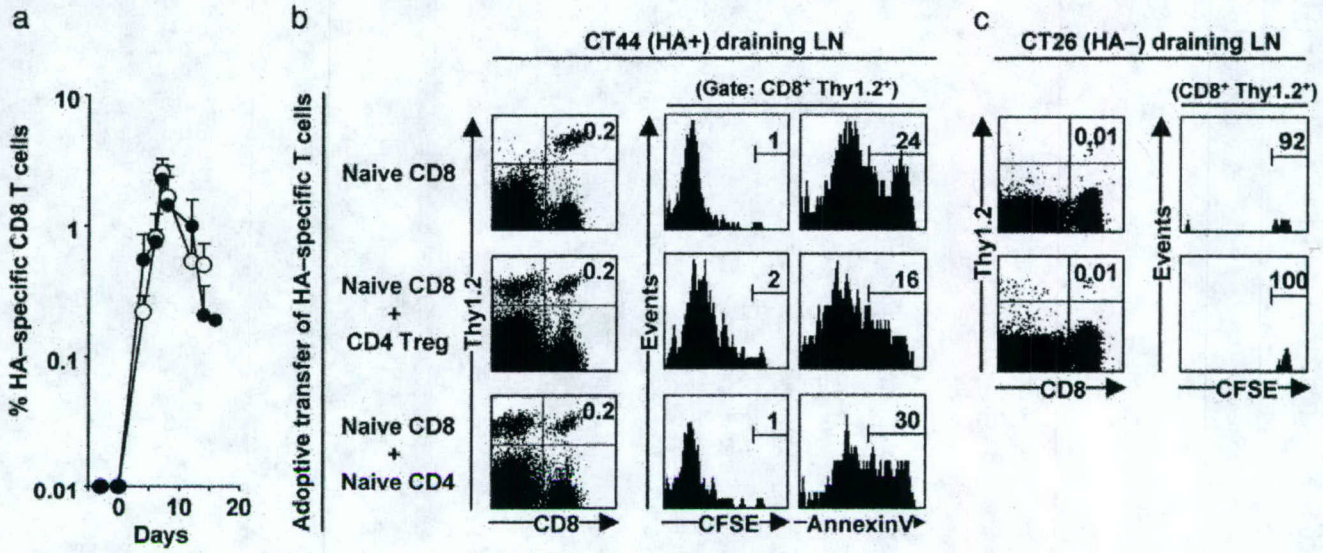

Fig. 2. HA-specific CD4 Treg neither impair proliferation nor accelerate apoptosis of HA-specific CD8 T cells. Thy1.1 BALB/c mice were adoptively transferred on day −1 with different combinations of CFSE-labeled Thy1.2 HA-specific T cells and challenged with CT26 (HA^-) and CT44 (HA^+) tumors on day 0 as described in Fig. 1. (*a*) CT44 draining LN from mice that received either naïve HA-specific CD8 T cells (○) or naïve HA-specific CD8 T cells and HA-specific CD4 Treg (●) were collected at different time points, and frequency of the transferred CD8 T cells (defined as $CD8^+Thy1.2^+$) was quantified by flow cytometry. (*b*) CD8 T cells in CT44 draining LN were assessed on day 6 for cell division (CFSE distribution) and apoptosis (binding to annexin V). (*c*) Similar analysis was performed with cells retrieved in CT26 tumor draining LN at the same time point. Similar results were obtained on days 4 and 8 (data not shown). Results show mean and SD values of six or more mice from at least three independent experiments.

observation that the dilution of CFSE label was not significantly different in CD8 cells expanding in the absence or presence of Treg (Fig. 2*b*). HA-specific CD4 Treg also accumulated within the same LN, starting from ≈0.01% of CD4 cells immediately after adoptive transfer (data not shown) and reaching 3.4 ± 0.8% of all LN CD4 cells on day 7 (Fig. 2*b*). HA-specific CD4 Treg accumulated slightly faster than HA-specific CD8 cells in CT44 draining LNs, because we found 2.8 ± 1.2 HA-specific Treg per HA-specific CD8 cell on day 7. Neither CD8 cells nor Treg accumulated in the LN draining the HA-negative CT26 tumor (Fig. 2*c*). HA-specific CD4 Treg did not accelerate apoptosis of HA-specific CD8 cells, because the vast majority of cells remained annexin V-negative in the presence or absence of Treg (Fig. 2*b*). Collectively, these data indicate that Treg did not interfere with the accumulation and division of tumor-specific CD8 cells in CT44 draining LN.

CD8 T Cell Differentiation Markers. In additional assays it was analyzed whether Treg interfered with the expression of differentiation cell surface molecules on HA-specific CD8 cells. To this end naïve HA-specific CD8 cells were adoptively transferred into BALB/c mice subsequently challenged with CT44. A significant fraction of Ag-primed HA-specific CD8 cells acquired an activated $CD25^+CD127^-CD69^+CD44^{high}CD62L^{low}$ phenotype, as demonstrated on day 7 in CT44 draining LN (see Fig. 6, which is published as supporting information on the PNAS web site). Similar phenotypic changes were observed when HA-specific CD8 cells were cotransferred with either naïve HA-specific CD4 cells or HA-specific CD4 Treg (Fig. 6). Because HA-specific CD8 cells acquired an activated phenotype irrespective of the absence or presence of Treg, expression of these markers could not be used as a diagnostic tool to predict survival of tumors.

CD8 T Cell Cytokines. Ag-primed effector CD8 cells release cytokines and lytic molecules that mediate a local inflammatory response and effect target cell apoptosis (29, 30). The influence of HA-specific Treg on the functional activity of CD8 cells was investigated by analyzing cytokine production in HA-specific CD8 cells on d 7 after tumor challenge. The majority of HA-specific CD8 cells produced IFN-γ and TNF-α upon restimulation with exogenous K_d-restricted $HA_{512–520}$ peptide or phorbol 12-myristate 13-acetate (PMA)/ionomycin (Fig. 3 *a–c* and Fig. 7, which is published as supporting information on the PNAS web site). Cotransfer of HA-specific CD4 Treg with HA-specific CD8 cells did not inhibit cytokine production. This

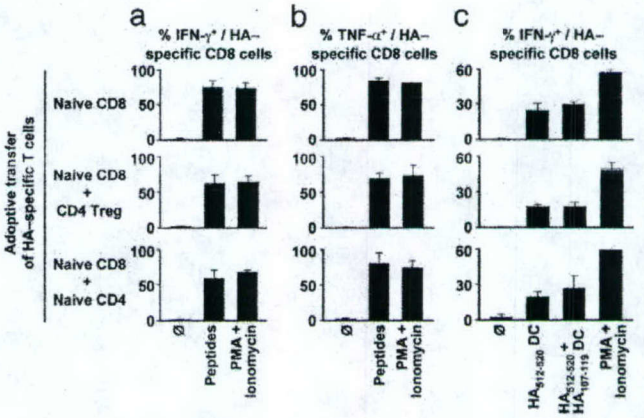

Fig. 3. HA-specific CD4 Treg do not control the production of inflammatory cytokines by HA-specific CD8 T cells. Thy1.1 BALB/c mice were adoptively transferred on day −1 with different combinations of Thy1.2 HA-specific T cells and challenged with CT44 (HA^+) tumors on day 0 as described in Fig. 1, from which CT44 draining LN cells were collected on day 6. HA-specific CD8 T cells were analyzed for IFN-γ (*a*) and TNF-α (*b*) production after 4-h restimulation with exogenously added $HA_{512–520}$ and $HA_{107–119}$ peptides or PMA/ionomycin. (*c*) HA-specific CD8 T cells were analyzed for IFN-γ production after 4-h restimulation with DCs previously pulsed with only $HA_{512–520}$ or both $HA_{512–520}$ and $HA_{107–119}$ peptides, or PMA/ionomycin. Results show mean and SD values of nine or more mice from at least three independent experiments.

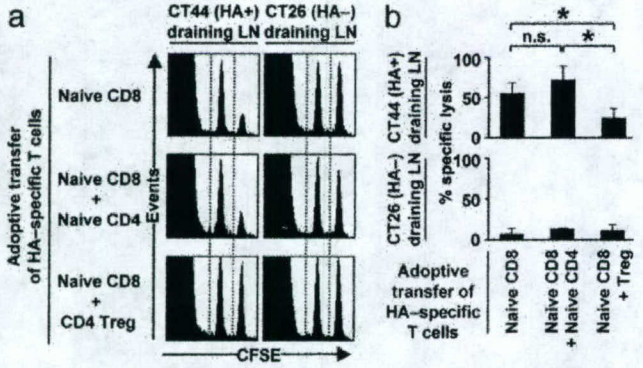

Fig. 4. HA-specific CD4 Treg suppress the cytotoxic activity of HA-specific CD8 T cells *in vivo*. BALB/c mice were adoptively transferred on day −1 with different combinations of HA-specific T cells and challenged with CT44 (HA$^+$) tumors on day 0 as described in Fig. 1. Mice were injected intravenously with a 1:1 mixture of syngeneic splenocytes previously labeled with 10 μM CFSE and pulsed with $HA_{512-520}$ peptide and of cells previously labeled with 1 μM CFSE but not pulsed with peptide. CT26 and CT44 draining LN were collected 16 h later, and Ag-specific killing of $HA_{512-520}$ positive targets was measured by flow cytometry. (*a*) Representative examples for *in vivo* killing of HA$^+$ targets. (*b*) Summary of *in vivo* killing of HA$^+$ targets. n.s., not significant; *, $P < 0.0001$. Results show mean and SD values of nine or more mice from at least three independent experiments.

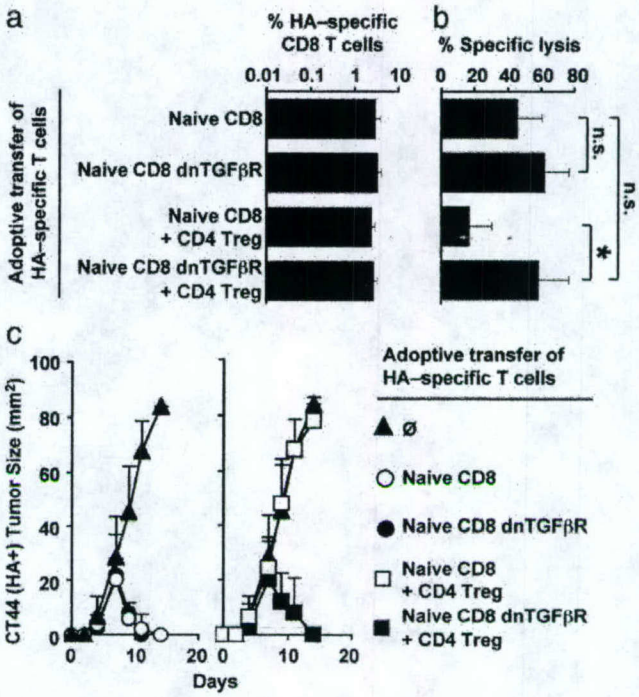

Fig. 5. Suppression of HA-specific CD8 T cell cytotoxic activity by HA-specific CD4 Treg requires TGF-β receptor signaling. On day −1, 10^5 naïve HA-specific CD8 T cells expressing or not expressing dnTGFβR were adoptively transferred into BALB/c mice either alone or with 10^5 HA-specific CD4 Treg. Mice were challenged with CT44 (HA$^+$) tumors on day 0. (*a*) HA-specific CD8 T cells in CT44 draining LN were quantified on day 6. (*b*) *In vivo* cytotoxic activity in CT44 draining LN was measured on day 6, as described in Fig. 4. n.s., not significant; *, $P < 0.0001$. (*c*) Tumor size was measured over a period of 2 wk in mice not receiving (*Left*) or receiving (*Right*) Treg. Results show mean and SD values of nine or more mice from at least three independent experiments.

result occurred whether the cells were restimulated only with class I MHC-restricted peptide, with both class I and class II MHC-restricted peptides, or with PMA and ionomycin, indicating that the reactivation of Treg *in vitro* did not suppress cytokine production by activated CD8 cells (Fig. 3 *a* and *b*).

We further investigated whether peptide presentation by K_d^+ I-E_d^+ antigen-presenting cells only (i.e., favoring close proximity of Treg and CD8 cells) could selectively impair CD8 T cell activity. To this end, purified splenic DCs (>97% CD11c$^+$ K_d^+ I-E_d^+) were pulsed with only the class I MHC-restricted peptide or with both class I and class II MHC-restricted peptides and used as antigen-presenting cells. Stimulation by PMA/ionomycin was used in controls. In the absence of HA-specific CD4 Treg, a significant fraction of HA-specific CD8 cells produced IFN-γ upon restimulation with peptide-pulsed DCs (Fig. 3*c*). This fraction was lower than the number of IFN-γ-producing HA-specific CD8 cells upon restimulation with PMA/ionomycin or with exogenously added HA peptide(s) (Fig. 3*a*). The difference is likely due to reduced Ag presentation when peptide-pulsed DCs were used (Fig. 3*c*) instead of supplying cultures with peptides without subsequent removal of nonbound peptide (Fig. 3 *a* and *b*). Importantly, the presence of HA-specific CD4 Treg did not interfere with cytokine production by CD8 cells even when the CD4 cells were restimulated with the class II MHC-restricted HA peptide (Fig. 3*c*). Collectively these experiments indicate that the Treg did not interfere with the ability of CD8 cells to produce IFN-γ at early stages of the immune response.

Suppression of CD8 T Cell Cytotoxicity. The cytotoxicity of HA-specific CD8 cells was addressed by *in vivo* readouts on day 6 after tumor challenge. In the absence of HA-specific CD4 Treg, HA-specific CD8 T cells specifically killed $HA_{512-520}$ peptide-pulsed targets in CT44 draining LNs but not in CT26 draining LNs. The presence of HA-specific CD4 Treg abolished the specific cytotoxic activity of HA-specific CD8 cells ($P < 0.0001$; Fig. 4). No *in vivo* killing of HA$^+$ targets was observed in popliteal LNs of nonchallenged mice or in CT44 draining LNs from CT44-bearing mice that did not receive HA-specific CD8 cells (data not shown). Importantly, because Treg did not interfere with the proliferation of naïve CD8 cells, the observed reduced cytotoxic activity in the presence of Treg in CT44 draining LNs indicates direct suppression of cytolytic activity rather than indirect suppression through impairment of proliferation.

TGF-β-Dependent Suppression. A potential role of TGF-β in the suppression of tumor rejection by CD8 cells was analyzed by introducing a dominant-negative TGF-β receptor into the tumor-specific CD8 cells, by crossing mice with the transgenic TCR specific for $K_d/HA_{512-520}$ with mice harboring a dnTGFβR (24). Expression of dnTGFβR by HA-specific CD8 cells did not alter their naïve phenotypic status at least in 4- to 6-wk-old animals, because the vast majority of both dnTGFβR and WT HA-specific CD8 cells were CD25$^-$CD127$^+$CD45RB^{high}CD69$^-$CD44^{low}CD62L^{high} (see Fig. 8, which is published as supporting information on the PNAS web site), whereas some dnTGFβR HA-specific CD8 cells in older animals (12–16 wk old) did exhibit the CD44 activation marker (data not shown). Therefore, CD8 cells used in further experiments were from 4- to 6-wk-old mice. When 10^5 naïve dnTGFβR or WT HA-specific CD8 cells were transferred into BALB/c mice, both populations of cells displayed similar kinetics of expansion in response to challenge with CT44 tumors (Fig. 5*a*) and rejected CT44 tumors (Fig. 5*c*). Thus, expression of the dnTGFβR in CD8 cells did not alter their expansion and the kinetic of tumor rejection. When coinjected with Treg, dnTGFβR and WT HA-specific CD8 cells also similarly expanded in response to challenge with CT44 tumors (Fig. 5*a*). However, expression of dnTGFβR by

HA-specific CD8 cells interfered with the suppression of tumor immunity by Treg because the kinetic of tumor rejection mediated by dnTGFβR HA-specific CD8 cells was comparable with the one mediated by WT HA-specific CD8 cells in the absence of Treg (Fig. 5*c*). To address whether this reaction resulted from a failure of Treg to suppress cytotoxicity, the effector function of dnTGFβR and WT CD8 cells in CT44 draining LN on day 7 was compared. Whereas the HA-specific CD8 cells efficiently lysed HA-peptide pulsed syngeneic target cells *in vivo* only in the absence of Treg, the cytotoxicity displayed by dnTGFβR HA-specific CD8 cells in the presence or absence of Treg was indistinguishable (Fig. 5*b*). Thus, expression of dnTGFβR by HA-specific CD8 cells was sufficient to render CD8 cells resistant to regulation by Treg and allowed efficient tumor rejection by cytolytic activity.

Discussion

This report describes the influence of HA-specific $CD4^+CD25^+$ Treg on the primary response of naïve HA-specific CD8 cells against HA-expressing tumors *in vivo*. The results show the following: (*i*) HA-specific CD8 cells were capable of rejecting HA-expressing tumors, whereas HA-negative tumors were not affected; (*ii*) HA-specific Treg effectively interfered with tumor rejection; (*iii*) suppression affected neither proliferation of CD8 cells during the first 10 days of the response nor the acquisition of a fully activated surface phenotype; (*iv*) suppression affected only the cytolytic activity of CD8 cells and had no impact on IFN-γ or TNF-α secretion; and (*v*) the molecular mechanism of CD8 suppression essentially involved TGF-β signaling because CD8 cells incapable of TGF-β signaling were resistant to suppression. Thus, Treg can effectively suppress the early tumor-specific immune response by CD8 cells by inhibiting their cytolytic activity in a TGF-β-dependent manner.

It has been shown that Treg can suppress the proliferation of CD4 and CD8 cells *in vitro* (3, 28, 31) and that *in vivo* Treg are capable of interfering with the proliferation of as well as production of IFN-γ by CD8 cells (8, 10, 12, 14). Indeed, secretion of IFN-γ by CD8 cells has been suggested to play a critical role in tumor rejection (32, 33). However, most of these studies have used polyclonal Treg where specific homing and expansion cannot be studied and no correlation between Ag-specific Treg and inhibition of CD8 cells can be made. Here, we have analyzed the impact of Treg on a primary CD8 immune response under conditions where CD8 cells and Treg have specificity for different peptides of the same protein expressed by tumor cells and where initially both naïve CD8 cells and Treg are present at a low frequency, as might be expected under physiological conditions. This procedure permits one to follow the Ag-specific responses of both cell types in the tumor draining LN and to correlate the mode of inhibition with local expansion. The data show that during the first week both the Ag-specific CD8 cells as well as the Ag-specific Treg home to and expand in the tumor draining LN and that the expanding Treg do not affect the proliferation of CD8 cells. Of interest is the observation that despite this finding, Treg interfere with tumor rejection by CD8 cells, which otherwise is complete by day 10 or shortly thereafter. Because suppression of proliferation could not explain these results, we analyzed whether Treg interfered with the effector functions of CD8 cells. Although no significant impairment of IFN-γ production was observed by day 7, there was an almost complete suppression of CD8-mediated cytolytic activity at this point in time. This suppression was essentially dependent on TGF-β signaling because CD8 cells with a dominant negative TGF-β receptor were resistant to suppression. This study also illustrates the importance of the Ag specificity of Treg on the control of CD8 cells, a feature of the immune system that is still poorly defined *in vivo*. It is noteworthy that the HA-specific CD8 cells were not controlled by the abundant $CD4^+CD25^+$ T cell repertoire endogenously present in the recipient mice, but were impaired selectively by lower numbers of HA-specific Treg, at least upon extensive Ag-specific proliferation.

We show that suppression of immune responses *in vivo* can occur by affecting distinct effector mechanisms at different stages of an immune response. In interpreting the results, one can envisage a scenario in which Treg and CD8 cells initially do not effectively interact with each other because of the low frequency of each population in the draining LN and, hence, physical separation of the two subsets. Thus, both populations expand significantly and thereby reach a frequency allowing a more effective interaction either directly or through Ag-presenting cell intermediates. It appears that at this stage, the suppression of cytolytic activity is more effective than the suppression of cytokine production or proliferation, i.e., cytotoxicity appears most sensitive to suppression, a notion consistent with observations by others that these effector functions can be regulated independently (27, 34–37), perhaps because they require different intensity of TCR signaling (38). Also, the cytokine requirement for proliferation of primary and memory CD8 cells may differ, and, hence, Treg may be more efficient in suppressing the proliferation of memory than of primary CD8 T cells. It is tempting to speculate that *in vivo* Treg-mediated suppression inhibits TCR signaling, the intensity of which controls different effector functions. This hypothesis could explain the reported suppression of CD8 T cell proliferation (8, 10) and/or IFN-γ secretion (9) in cases of viral or bacterial infection, under conditions in which the ratio of Ag-specific Treg and CD8 cells is unknown. Our results also show that in this model of tumor rejection, loss of cytolytic activity is sufficient to allow tumor outgrowth even when tumor-specific T cells still produce high levels of IFN-γ.

Independent evidence suggests that the suppression of CD8 T cell cytotoxicity by Treg may be common in cancer. It is of interest that tumor-specific CD8 cells frequently accumulate in tumors of melanoma patients but fail to exert cytolytic effector function (15), especially under conditions where tumor-specific CD4 Treg also could be identified within the tumor stroma (16, 17). These observations are consistent with results described in this study showing that tumor-specific CD4 Treg did not perturb the proliferation of HA-specific CD8 cells but suppressed their cytolytic activity *in vivo*. Such suppression may not only occur in draining LN but also among extravasated CD4 and CD8 cells within the tumor. In this context, it is of considerable interest that the pathway of immune suppression of cytolytic activity essentially depends on signaling by the TGF-β receptor on CD8 cells. Although previous studies on TGF-β-mediated inhibition have not addressed specific effector functions (20), our observations provide a rational explanation for earlier findings indicating that T-cell-specific blockade of TGF-β signaling renders mice resistant to tumors that otherwise would have been lethal (39). TGF-β-mediated suppression of CD8 T cell cytolytic activity *in vitro* has been studied by several investigators, and it has been reported by some that TGF-β interferes at early phases of the cytotoxic response but is rather ineffective once cells have developed cytolytic activity (40). However, there are also studies describing a more direct inhibition of cytolytic activity by TGF-β by interfering with the production of pore-forming protein independently of proliferation (41) that are consistent with our observations. Our results, thus, show that under conditions where the homing and accumulation of Ag-specific T cells and their CD8 targets can be tightly monitored, it is possible to identify a specific effector CD8 T cell function, namely cytolytic activity, that is most susceptible to TGF-β-mediated inhibition of regulatory T cells.

We thank Ludger Klein for critical suggestions, Silke Paust for discussions, Thorsten Mempel (CBR Institute, Harvard Medical School) and Glenn Dranoff (Dana–Farber Cancer Institute, Harvard Medical School) for providing us Flt3L-expressing tumor cells and advice, and Dina Lazik for excellent technical assistance. M.L.C. was supported by

a Cancer Research Institute Investigator Award in Cancer Immunology; M.P. was supported by Swiss National Foundation Grant PBLAB-100856 and Human Frontier Science Program Organization Grant LT00369/2003; and K.K. was supported by Ruth L. Kirschstein National Research Service Award R33 CA97728-02 and Idea Award DAMD17-02-1-0361.

1. Shevach, E. M. (2004) *Semin. Immunol.* **16,** 69–71.
2. Sakaguchi, S. (2004) *Annu. Rev. Immunol.* **22,** 531–562.
3. Suri-Payer, E., Amar, A. Z., Thornton, A. M. & Shevach, E. M. (1998) *J. Immunol.* **160,** 1212–1218.
4. von Boehmer, H. (2003) *J. Exp. Med.* **198,** 845–849.
5. Walker, L. S., Chodos, A., Eggena, M., Dooms, H. & Abbas, A. K. (2003) *J. Exp. Med.* **198,** 249–258.
6. Fisson, S., Darrasse-Jeze, G., Litvinova, E., Septier, F., Klatzmann, D., Liblau, R. & Salomon, B. L. (2003) *J. Exp. Med.* **198,** 737–746.
7. Yamazaki, S., Iyoda, T., Tarbell, K., Olson, K., Velinzon, K., Inaba, K. & Steinman, R. M. (2003) *J. Exp. Med.* **198,** 235–247.
8. Suvas, S., Kumaraguru, U., Pack, C. D., Lee, S. & Rouse, B. T. (2003) *J. Exp. Med.* **198,** 889–901.
9. Dittmer, U., He, H., Messer, R. J., Schimmer, S., Olbrich, A. R., Ohlen, C., Greenberg, P. D., Stromnes, I. M., Iwashiro, M., Sakaguchi, S., *et al.* (2004) *Immunity* **20,** 293–303.
10. Kursar, M., Bonhagen, K., Fensterle, J., Kohler, A., Hurwitz, R., Kamradt, T., Kaufmann, S. H. & Mittrucker, H. W. (2002) *J. Exp. Med.* **196,** 1585–1592.
11. Lin, C. Y., Graca, L., Cobbold, S. P. & Waldmann, H. (2002) *Nat. Immunol.* **3,** 1208–1213.
12. Dai, Z., Li, Q., Wang, Y., Gao, G., Diggs, L. S., Tellides, G. & Lakkis, F. G. (2004) *J. Clin. Invest.* **113,** 310–317.
13. Malek, T. R., Yu, A., Vincek, V., Scibelli, P. & Kong, L. (2002) *Immunity* **17,** 167–178.
14. Murakami, M., Sakamoto, A., Bender, J., Kappler, J. & Marrack, P. (2002) *Proc. Natl. Acad. Sci. USA* **99,** 8832–8837.
15. Zippelius, A., Batard, P., Rubio-Godoy, V., Bioley, G., Lienard, D., Lejeune, F., Rimoldi, D., Guillaume, P., Meidenbauer, N., Mackensen, A., *et al.* (2004) *Cancer Res.* **64,** 2865–2873.
16. Wang, H. Y., Lee, D. A., Peng, G., Guo, Z., Li, Y., Kiniwa, Y., Shevach, E. M. & Wang, R. F. (2004) *Immunity* **20,** 107–118.
17. Curiel, T. J., Coukos, G., Zou, L., Alvarez, X., Cheng, P., Mottram, P., Evdemon-Hogan, M., Conejo-Garcia, J. R., Zhang, L., Burow, M., *et al.* (2004) *Nat. Med.* **10,** 942–949.
18. Piccirillo, C. A., Letterio, J. J., Thornton, A. M., McHugh, R. S., Mamura, M., Mizuhara, H. & Shevach, E. M. (2002) *J. Exp. Med.* **196,** 237–246.
19. Peng, Y., Laouar, Y., Li, M. O., Green, E. A. & Flavell, R. A. (2004) *Proc. Natl. Acad. Sci. USA* **101,** 4572–4577.
20. Green, E. A., Gorelik, L., McGregor, C. M., Tran, E. H. & Flavell, R. A. (2003) *Proc. Natl. Acad. Sci. USA* **100,** 10878–10883.
21. Kirberg, J., Baron, A., Jakob, S., Rolink, A., Karjalainen, K. & von Boehmer, H. (1994) *J. Exp. Med.* **180,** 25–34.
22. Morgan, D. J., Liblau, R., Scott, B., Fleck, S., McDevitt, H. O., Sarvetnick, N., Lo, D. & Sherman, L. A. (1996) *J. Immunol.* **157,** 978–983.
23. Klein, L., Trautman, L., Psarras, S., Schnell, S., Siermann, A., Liblau, R., von Boehmer, H. & Khazaie, K. (2003) *Eur. J. Immunol.* **33,** 806–814.
24. Gorelik, L. & Flavell, R. A. (2000) *Immunity* **12,** 171–181.
25. Mora, J. R., Bono, M. R., Manjunath, N., Weninger, W., Cavanagh, L. L., Rosemblatt, M. & Von Andrian, U. H. (2003) *Nature* **424,** 88–93.
26. Klein, L., Khazaie, K. & von Boehmer, H. (2003) *Proc. Natl. Acad. Sci. USA* **100,** 8886–8891.
27. Lyman, M. A., Aung, S., Biggs, J. A. & Sherman, L. A. (2004) *J. Immunol.* **172,** 6558–6567.
28. Piccirillo, C. A. & Shevach, E. M. (2001) *J. Immunol.* **167,** 1137–1140.
29. Trapani, J. A. & Smyth, M. J. (2002) *Nat. Rev. Immunol.* **2,** 735–747.
30. Shankaran, V., Ikeda, H., Bruce, A. T., White, J. M., Swanson, P. E., Old, L. J. & Schreiber, R. D. (2001) *Nature* **410,** 1107–1111.
31. Somasundaram, R., Jacob, L., Swoboda, R., Caputo, L., Song, H., Basak, S., Monos, D., Peritt, D., Marincola, F., Cai, D., *et al.* (2002) *Cancer Res.* **62,** 5267–5272.
32. Qin, Z., Schwartzkopff, J., Pradera, F., Kammertoens, T., Seliger, B., Pircher, H. & Blankenstein, T. (2003) *Cancer Res.* **63,** 4095–4100.
33. Blankenstein, T. & Qin, Z. (2003) *Curr. Opin. Immunol.* **15,** 148–154.
34. Veiga-Fernandes, H., Walter, U., Bourgeois, C., McLean, A. & Rocha, B. (2000) *Nat. Immunol.* **1,** 47–53.
35. Snyder, J. E., Bowers, W. J., Livingstone, A. M., Lee, F. E., Federoff, H. J. & Mosmann, T. R. (2003) *Nat. Med.* **9,** 231–235.
36. Hernandez, J., Aung, S., Marquardt, K. & Sherman, L. A. (2002) *J. Exp. Med.* **196,** 323–333.
37. Apostolou, I., Sarukhan, A., Klein, L. & von Boehmer, H. (2002) *Nat. Immunol.* **3,** 756–763.
38. Valitutti, S., Muller, S., Dessing, M. & Lanzavecchia, A. (1996) *J. Exp. Med.* **183,** 1917–1921.
39. Gorelik, L. & Flavell, R. A. (2001) *Nat. Med.* **7,** 1118–1122.
40. Erard, F., Garcia-Sanz, J. A., Moriggl, R. & Wild, M. T. (1999) *J. Immunol.* **162,** 209–214.
41. Smyth, M. J., Strobl, S. L., Young, H. A., Ortaldo, J. R. & Ochoa, A. C. (1991) *J. Immunol.* **146,** 3289–3297.

In vivo dynamics of antigen-specific regulatory T cells not predicted from behavior *in vitro*

Ludger Klein*, Khashayarsha Khazaie, and Harald von Boehmer†

Harvard Medical School, Dana–Farber Cancer Institute, 44 Binney Street, Smith 736, Boston, MA 02115

Communicated by Klaus Rajewsky, Harvard Medical School, Boston, MA, June 3, 2003 (received for review May 13, 2003)

Adoptive transfer of antigen-specific CD25$^+$CD4$^+$ regulatory T cells was used to analyze the stability of their phenotype, their behavior after immunization, and their mode of suppressing cotransferred naive T cells *in vivo*. We found that regulatory T cells maintained their phenotype in the absence of antigen, were not anergic *in vivo*, and proliferated as extensively as naive CD4$^+$ T cells after immunization without losing their suppressive function *in vivo* and *in vitro*. *In vivo*, the expansion of cotransferred naive T cells was suppressed relatively late in the response such that regulatory T cells expressing mostly IL-10 but not IL-2 or IFN-γ represented the dominant subset of cells. Our results reveal properties of regulatory T cells that were not predicted from *in vitro* studies.

Dominant mechanisms of tolerance control the autoimmune potential of self-reactive T cells in healthy individuals and animals (reviewed in refs. 1–3). Insights into the regulation of immune responses by regulatory T cells have been mostly obtained with polyclonal populations of regulatory T cells for which the role of specific antigen has been largely obscure. The impact of self-antigen on the shaping of the regulatory T cell pool came more into focus when it was observed that the coexpression of a transgenic class II MHC restricted T cell receptor (TCR) and its agonist ligand resulted in the generation of antigen-specific regulatory T cells (4). Subsequent experiments in that system confirmed the notion that thymic epithelium can have a decisive role in the formation of such cells by demonstrating that the expression of an agonist ligand on radioresistant tissue (5) and on transplanted thymic epithelium (6) was a very effective means of generating regulatory T cells, whereas the mode of generation of polyclonal regulatory T cells in normal mice still needs to be elucidated.

A subset of CD4$^+$ T cells expressing the interleukin-2 (IL-2) receptor α-chain (CD25) recently became a major focus of interest. These CD4$^+$CD25$^+$ T cells were first shown by Sakaguchi and colleagues to control autoreactive T cells *in vivo* (7). Several characteristics of these cells have emerged from *in vitro* studies (reviewed in ref. 8) resulting in the notion that regulatory T cells are anergic in terms of proliferation and suppress other cells by direct cell contact, which requires neither IL-10 nor transforming growth factor-β and which results in the inability of suppressed CD4$^+$ T cells to produce IL-2 (9–11). However, it is unclear at present how far these observations *in vitro* are in fact a reflection of the properties of CD4$^+$CD25$^+$ T cells *in vivo*. In some experimental systems of immune regulation by CD4$^+$CD25$^+$ T cells *in vivo*, it was found that soluble factors such as IL-4, IL-10, and transforming growth factor-β do contribute to the prevention of autoimmunity, with the role of these factors varying between different models (12–14). Polyclonal CD25$^+$CD4$^+$ T cells proliferate and expand when they are transferred into *rag*$^{-/-}$ or IL-2 receptor β-deficient mice (15–17), indicating that their anergic state can be reversed under certain nonphysiological conditions. Notably, it is under exactly these lymphopenic conditions that the regulatory function of CD25$^+$CD4$^+$ T cells has been studied in the majority of the currently available models, at least suggesting that proliferation and suppressive function by regulatory T cells may not be mutually exclusive. A major experimental drawback of lymphopenic models of immune regulation, however, is that they provide no information on antigen-induced proliferation as observed in nonlymphopenic mice.

The present study was initiated to establish an *in vivo* system of antigen-specific immune regulation that is as physiological as possible to characterize the behavior of CD25$^+$CD4$^+$ regulatory T cells at relatively low frequency in the context of an unperturbed immune system. To this end, TCR transgenic CD25$^+$CD4$^+$ T cells were adoptively transferred into normal hosts either alone or in combination with naive CD4$^+$25$^-$ T cells of identical antigen specificity. Immunization with cognate antigen was used to visualize and compare the behavior of the respective populations either alone or in combination.

Materials and Methods

Mice and Transgenic Vectors. BALB/c Thy1.2 mice were purchased from Taconic Farms. Other strains were bred in the animal facility of the Dana–Farber Cancer Institute under specific pathogen-free conditions.

Phosphoglycerate kinase-hemagglutinin (*pgk-HA*) mice were generated through germ-line cre-mediated recombination in mice carrying a *pgk-*^{lox}*β-gal*^{lox}*-HA* cassette vector. This vector was constructed as follows. Lox P sites were introduced 5′ and 3′ of the *β-gal* cDNA. The HA cDNA then was introduced downstream of the 3′ lox P site, and the construct was cloned into a eukaryotic expression vector driven by the *pgk* promoter. Transgenic founders (F_1 FVB × 129) were backcrossed to BALB/c for at least five generations before being crossed to TS4 cre mice (18) or Whey acidic protein-cre mice (19) that had been backcrossed to BALB/c for at least four generations. Both crosses unexpectedly led to germ-line recombination of the transgene. Germ-line-recombined mice then were maintained by further backcrossing of *pgk-HA* × *TCR-HA* double-transgenic mice to BALB/c for at least four generations.

Immunization. Mice were immunized s.c. with 100 μg of peptide HA$^{107–119}$ emulsified in incomplete Freund's adjuvant (IFA, Sigma–Aldrich). At the indicated time points the animals were killed, and draining (popliteal and inguinal) and distant (mesenteric) lymph nodes were harvested for analysis. The tumor cell line CT26 HA-EGFP has been described elsewhere (20).

Antibodies and Fluorescence-Activated Cell Sorter Analysis. Biotin-conjugated mAbs to CD4 (H129.19) and Thy1.1 (HIS51), phycoerythrin-conjugated mAbs to CD4 (GK1.5), CD25 (PC61), IL-2 (JES6–5H4), IL-10 (JES5-16E3), IFN-γ (XMG.1.2), tumor necrosis factor α (MP6-XT22), rat IgG_1 isotype control (R3-34), and rat IgG_{2b} isotype control (A95-1), Cy-chrome-conjugated streptavidin, mAbs to CD8 (53-6.7), and allophycocyanin-conjugated mAbs to CD4 (RM4-5), CD25 (PC61), and Thy1.2

Abbreviations: TCR, T cell receptor; pgk, phosphoglycerate kinase; HA, hemagglutinin; IFA, incomplete Freund's adjuvant; CFSE, 5,6-carboxyfluorescein diacetate-succinimidyl ester.

*Present address: Research Institute of Molecular Pathology, Dr. Bohr-Gasse 7, A-1030 Vienna, Austria.

†To whom correspondence should be addressed. E-mail: harald_von_boehmer@dfci.harvard.edu.

www.pnas.org/cgi/doi/10.1073/pnas.1533365100

(53-2.1) were purchased from Becton Dickinson. The mAb to the *TCR-HA* (6.5) was purified and conjugated with FITC in our lab. Fc-receptor-blocking mAb 2.4G2 was used as culture supernatant. Surface stainings were performed according to standard procedures at a density of $2–4 \times 10^6$ cells per 50 μl, and volumes were scaled up accordingly. Flow-cytometric analysis was performed on a FACSCalibur (Becton Dickinson) by using CELLQUEST software (Becton Dickinson).

Intracellular Cytokine Staining. Cells from the draining lymph node of immunized animals were resuspended at a density of 2×10^6 cells per ml in Iscove's modified Dulbecco's medium containing 10% FCS. Cells then were plated in 6 ml per well into six-well culture plates, 12 μl of leukocyte activation mixture with GolgiPlug (Becton Dickinson) containing phorbol 12-myristate 13-acetate, ionomycin, and brefeldin A were added, and cultures were incubated at 37°C for 6 h. Cells were harvested and incubated with 2.4G2 Fc-receptor-blocking antibody before surface staining. Cells then were fixed with Cytofix/Cytoperm buffer (Becton Dickinson) for 20 min at room temperature. Intracellular cytokine staining was performed at room temperature for 20 min in Perm/Wash buffer (Becton Dickinson). Control stainings were performed with a mixture of phycoerythrin-conjugated isotype controls.

Purification and Adoptive Transfer of Cells. Pooled cells from spleen and peripheral lymph nodes (mesenteric, axillary, brachial, popliteal, inguinal, and cervical) from *pgk-HA* × *TCR-HA* mice were subjected to erythrocyte lysis. Cells then were incubated with Fc-receptor-blocking antibody 2.4G2 and stained with anti-CD4 biotin. After incubation with streptavidin microbeads (Miltenyi Biotec, Auburn, CA), $CD4^+$ cells were positively selected on midi-MACS columns, routinely achieving purities >95%. Cells then were stained with streptavidin-Cy-chrome, anti-CD25 phycoerythrin, and FLUOS-labeled 6.5. $CD4^+CD25^+6.5^+$ cells were sorted by using a MoFlow cell sorter (Cytomation, Fort Collins, CO). Naive *TCR-HA* $CD4^+$ T cells were obtained from spleen and lymph nodes of *TCR-HA* $rag^{-/-}$ mice by magnetic enrichment for CD4 T cells.

Cells were injected into the lateral tail vein in a volume of 200 μl of PBS. Where indicated, cells were labeled with 5,6-carboxyfluorescein diacetate-succinimidyl ester (CFSE) (Molecular Probes) by incubation for 10 min at 37°C in 10 μM CFSE in PBS/0.1% BSA at a density of 1×10^7 cells per ml.

Proliferation Assays. For inhibition assays, 2×10^4 sorted or magnetically enriched $CD25^+$ and/or $CD25^-$ $CD4^+6.5^+$ T cells were incubated with 2×10^5 irradiated (3,000 rad) BALB/c splenocytes in the presence of 5 μg/ml $HA^{107–119}$ peptide in 200 μl of Iscove's modified Dulbecco's medium supplemented with 10% FCS in 96-well round-bottom plates. Where indicated, 50 units/ml recombinant IL-2 were added (Becton Dickinson). Proliferation was measured by scintillation counting after pulsing with 1 μCi per well [^{3}H]thymidine (1 Ci = 37 GBq) for the last 16–20 h of a 90-h incubation period.

For *ex vivo* proliferation assays, cells from draining lymph nodes were cultured for 72–90 h in triplicates at 4×10^5 cells per well in round-bottom 96-well plates in serum-free medium (HL-1, BioWhittaker). Proliferation was measured as incorporation of [^{3}H]thymidine, which was added for the last 18 h of culture (1 μCi per well).

Results

High Frequency of Antigen-Specific $CD25^+CD4^+$ Regulatory T Cells in *pgk-HA* × *TCR-HA* Mice. Mice expressing influenza-HA under the control of the ubiquitous *pgk* promoter, in the following referred to as *pgk-HA* mice, were crossed to mice expressing a transgenic TCR (*TCR-HA*) specific for peptide 111–119 of HA (21). Among lymph node cells of *pgk-HA* × *TCR-HA* mice, the fraction of $CD4^+$ $TCR\text{-}HA^+$ cells was reduced by a factor of 2 as assessed by staining with the anti-clonotypic antibody 6.5, and a distinct population of 6.5^+CD25^+ cells that could not be detected in TCR single transgenics was observed (Fig. 1*a*). Sorted 6.5^+CD25^+ cells from thymus (Fig. 7, which is published as supporting information on the PNAS web site, www.pnas.org) or periphery (Fig. 1*b*) of double-transgenic mice were anergic *in vitro* and suppressed the proliferation of naive 6.5^+CD4^+ T cells in standard coculture assays. The addition of IL-2 enabled proliferation of 6.5^+CD25^+ cells from both thymus and periphery (data not shown). Thymus transplantation revealed that expression of HA by radioresistant thymic epithelium was sufficient to mediate the selection of 6.5^+CD25^+ cells (data not shown). Thus, by these criteria, the HA-specific $CD25^+$ cells were equivalent to polyclonal $CD25^+$ suppressor T cells from normal mice.

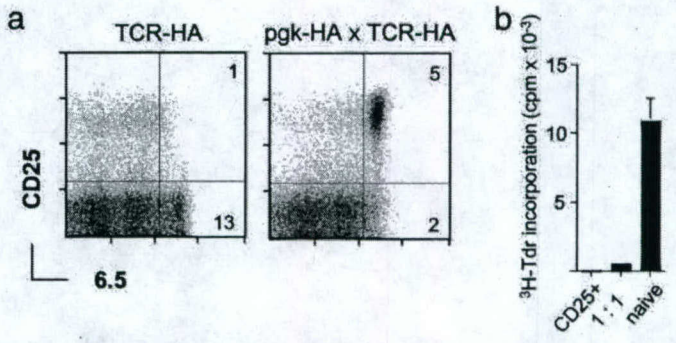

Fig. 1. High frequency of HA-specific regulatory $CD4^+CD25^+$ T cells in *pgk-HA* × *TCR-HA* mice. (*a*) Expression of the transgenic TCR (mAb 6.5) versus CD25 on gated CD4 T cells from lymph nodes of *TCR-HA* single-transgenic versus *pgk-HA* × *TCR-HA* double-transgenic mice. Numbers in the dot plots indicate the percentage of gated cells within the respective quadrants. (*b*) $CD25^+$ CD4 T cells from *pgk-HA* × *TCR-HA* mice were anergic and suppressed the proliferation of naive CD4 T cells from *TCR-HA* $rag^{-/-}$ mice *in vitro*. Sorted $CD4^+CD25^+6.5^+$ cells from *pgk-HA* × *TCR-HA* mice and naive $CD4^+6.5^+$ T cells from *TCR-HA* $rag^{-/-}$ mice were incubated either alone or together (ratio 1:1) in the presence of BALB/c splenocytes and HA-peptide for 90 h. Proliferation was measured as incorporation of [^{3}H]thymidine (^{3}H-Tdr) added for the last 20 h.

Suppression of Anti-HA Responses *in Vivo* After Transfer of $CD25^+$ Regulatory T Cells. 6.5^+CD25^+ CD4 T cells from *pgk-HA* × *TCR-HA* $Thy1.2^+$ mice were transferred into $Thy1.1^+$ hosts. The frequency of donor-derived cells among host cells was similar when equal numbers of either $CD25^+$ cells from *pgk-HA* × *TCR-HA* mice or naive 6.5^+CD25^- cells from *TCR-HA* $rag^{-/-}$ mice were transferred. Fourteen days after transfer, most (>85%) donor-derived cells still expressed the CD25 marker, and their number appeared stable within this time frame (data not shown). Reisolated cells were still anergic and suppressed naive 6.5^+ CD4 T cells *in vitro* (Fig. 2 *a* and *b*), indicating that they represented a lineage rather than antigen-dependent effector cells.

We next asked whether transferred 6.5^+CD25^+ cells could inhibit the response of endogenous HA-specific T cells. Recipients of 3×10^5 6.5^+CD25^+ cells, corresponding to a frequency of approximately 1 in 3,000 $CD4^+$ T cells, or noninjected control mice were immunized with peptide $HA^{107–119}$ in IFA. Although draining lymph node cells from control animals proliferated vigorously when restimulated *in vitro*, no proliferation was detected with cells from recipients of regulatory T cells (Fig. 2*c*).

The colon carcinoma cell line CT26-HA, which stably expresses HA (20), was used to test whether transferred 6.5^+CD25^+ cells influenced the growth of an HA-expressing

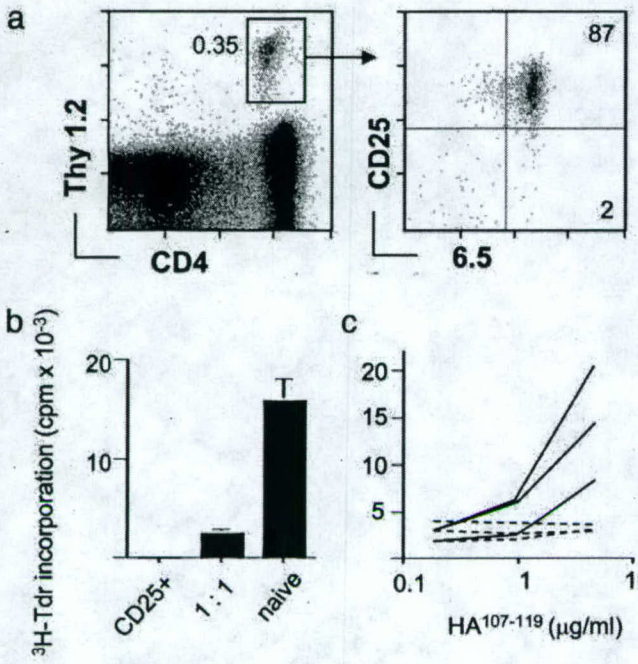

Fig. 2. Transferred CD4$^+$CD25$^+$6.5$^+$ T cells retain their phenotypic and *in vitro* regulatory properties in the absence of antigen and suppress endogenous anti-HA-specific T cells after immunization. (*a*) CD4$^+$CD25$^+$6.5$^+$ T cells (4×10^6) from Thy1.2$^{+/+}$ *pgk-HA* × *TCR-HA* mice were transferred into BALB/c Thy1.1$^{+/+}$ mice. Six days after transfer, the recipients were killed. Peripheral lymph nodes and spleen were pooled and stained for CD4, Thy1.2, CD25, and 6.5. The frequency of donor-derived cells among CD4 T cells is shown together with the sorting gate used for reisolation of cells. (*Right*) Purity of reisolated cells. (*b*) Reisolated Thy1.2$^{+/+}$ cells 6 days after transfer were tested for their proliferative response after stimulation with HA-peptide and their suppressive potential when cocultured with naive cells as described for Fig. 1. (*c*) Recipients of 3×10^5 CD4$^+$CD25$^+$6.5$^+$ T cells (dashed lines) or untreated BALB/c mice (solid lines) were immunized with HA-peptide (100 μg) in IFA. Eight days later, draining lymph node cells were harvested and stimulated *in vitro* with titrated amounts of HA-peptide for 90 h. Incorporation of [^{3}H]thymidine (^{3}H-Tdr) within the last 20 h was measured. The graph shows the data for three immunized mice of each group representative for three independent experiments.

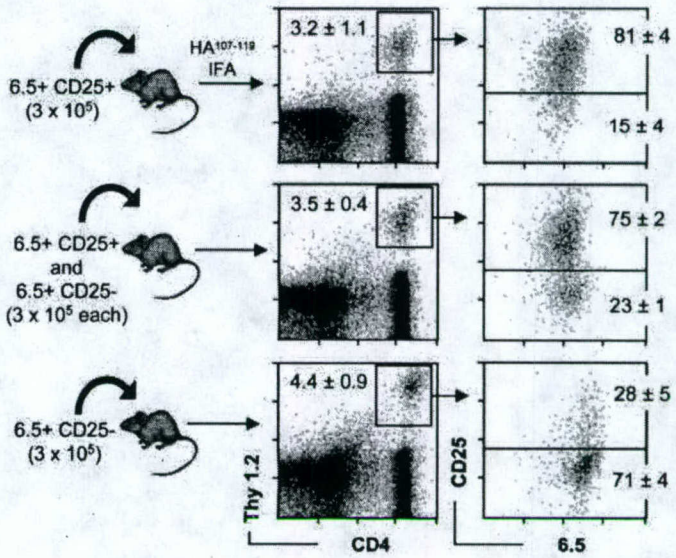

Fig. 3. Accumulation of CD4$^+$CD25$^+$6.5$^+$ T cells or naive CD4$^+$CD25$^-$6.5$^+$ T cells in the draining lymph nodes after immunization. (*a*) Thy1.1$^{+/+}$ recipients of CD4$^+$CD25$^+$6.5$^+$ T cells, CD4$^+$CD25$^-$6.5$^+$ T cells, or both types of cells were immunized with HA-peptide as described for Fig. 2. Draining lymph node cells were harvested on day 8 after immunization and stained for CD4, Thy1.2, CD25, and 6.5. (*Left*) Numbers in the dot plots indicate the percentage of donor-derived cells among CD4$^+$ T cells (mean of four animals). (*Right*) The dot plots show the expression of the transgenic TCR (6.5) versus CD25 on gated CD4$^+$Thy1.2$^+$ cells. Numbers within the dot plots indicate the percentage of gated cells in the respective quadrant (mean of four animals).

tumor by suppressing the antitumor response. Subcutaneous inoculation of normal BALB/c mice with CT26-HA leads to the induction of anti-HA CD4 and CD8 T cell responses (20). Transfer of 6.5$^+$CD25$^+$ cells allowed for accelerated growth of the tumor (Fig. 8, which is published as supporting information on the PNAS web site). Furthermore, although in tumor-bearing normal mice or mice that had received naive CD25$^-$ 6.5$^+$ CD4 T cells a strong *ex vivo* proliferative response was observed, such a recall response was absent with cells from recipients of CD25$^+$ 6.5$^+$ T cells irrespective of whether naive cells had been cotransferred (Fig. 8). Thus, transferred CD25$^+$ cells had potent suppressive activity *in vivo*.

Antigen-Driven Expansion of CD25$^+$CD4$^+$ T Cells *in Vivo*. We next aimed to visualize and compare the behavior of antigen-specific regulatory and naive T cells after immunization. A control group received 3×10^5 6.5$^+$CD25$^-$ cells only and was immunized the following day. On day 8 after immunization, ≈4% of draining lymph node CD4 T cells were donor-derived, and the majority of these cells was CD25$^-$ (Fig. 3). In nondraining lymphoid compartments, <0.05% of CD4 T cells were Thy1.2$^+$, similar to the values observed in nonimmunized recipients (data not shown). Thus, HA-specific "naive" T cells expectedly increased ≈100-fold in the antigen-exposed lymph node. A second group of animals received 3×10^5 6.5$^+$CD25$^+$ cells and was immunized and analyzed as described above. Surprisingly, we found a distribution of donor-derived cells in these animals very similar to that observed in recipients of naive cells. Approximately 3% of CD4 T cells in the draining lymph nodes were donor-derived, whereas in distant lymphoid compartments, <0.05% of CD4 T cells were Thy1.2$^+$ (data not shown). Contrary to recipients of naive cells, these cells mostly expressed the CD25 marker (Fig. 3). A third group received both 6.5$^+$CD25$^+$ and naive 6.5$^+$CD25$^-$ cells. Eight days after immunization the proportion of donor-derived cells among CD4 T cells in the draining lymph node was again ≈3%, and the majority of these cells expressed high levels of CD25, as was observed in mice that had received 6.5$^+$CD25$^+$ cells only (Fig. 3).

The almost identical frequencies of donor-derived cells in the draining lymph nodes of recipients of either regulatory or naive T cells implied a similar homing/expansion pattern of both cell types, a surprising finding considering the absence of an *in vitro* recall response in recipients of CD25$^+$ T cells (see Fig. 2*c*). To confirm this apparent discrepancy, we restimulated draining lymph node cells from the three groups with HA-peptide *in vitro*. Cells from recipients of naive cells showed a very strong response, whereas neither recipients of 6.5$^+$CD25$^+$ cells alone nor recipients of mixed populations displayed any antigen-specific *in vitro* proliferation (data not shown).

To address whether antigen-driven expansion *in vivo* altered the properties of 6.5$^+$CD25$^+$ cells *in vitro*, we sorted these cells from draining lymph nodes of immunized recipients and compared them with 6.5$^+$CD25$^+$ cells taken directly from *pgk-HA* × *TCR-HA* mice. When stimulated *in vitro*, both populations were completely anergic with respect to proliferation, and provision of IL-2 restored some proliferation in both types of cultures, yet less efficiently with "expanded regulators" (data not shown). When titrated in the standard coculture assay, expanded regulators were ≈4-fold more efficient suppressors than "nonexpanded

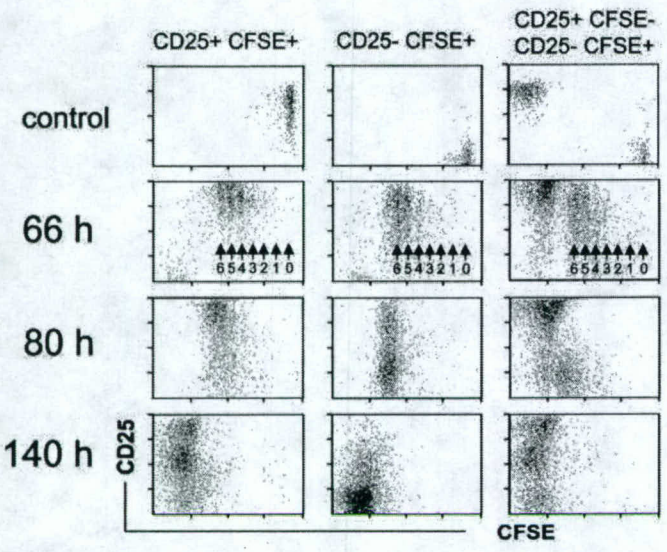

Fig. 4. Proliferation of adoptively transferred $CD4^+CD25^+6.5^+$ T cells or $CD4^+CD25^-6.5^+$ T cells in the draining lymph nodes after immunization. CFSE-labeled $CD4^+CD25^+6.5^+$ T cells from *pgk-HA* × *TCR-HA* mice (3×10^5) (*Left*) or CFSE-labeled naive $CD4^+CD25^-6.5^+$ T cells from *TCR-HA rag*$^{-/-}$ mice (3×10^5) were transferred into BALB/c Thy1.1 mice. Two days later, recipients were immunized with 100 μg of HA-peptide in IFA. Controls were immunized with IFA without peptide. Mice were killed at the indicated time points after immunization, and draining lymph node cells were harvested and stained for CD4, Thy1.2, and CD25. The dot plots show the expression of CD25 versus CFSE fluorescence intensity on gated donor-derived cells ($CD4^+Thy1.2^+$). Numbered arrows within the dot plots (66 h) indicate the number of divisions of CFSE-labeled cells. Note that all dot plots (except controls, where ≈200 events are shown) show 800–1,000 $CD4^+Thy1.2^+$ events and thus do not represent the frequency of these cells among host CD4 T cells. (*Right*) Representative analysis of a cotransfer of 3×10^5 CFSE-labeled naive $CD4^+CD25^-6.5^+$ T cells from *TCR-HA rag*$^{-/-}$ mice and 3×10^5 unlabeled $CD4^+CD25^+6.5^+$ T cells from *pgk-HA* × *TCR-HA* mice into BALB/c Thy1.1 recipients.

regulators" (Fig. 9, which is published as supporting information on the PNAS web site).

$CD25^+$ Regulatory T Cells Do Not Affect the Initial Expansion of Naive Cells After Immunization. To address whether the accumulation of 6.5^+CD25^+ cells in the draining lymph nodes was a result of proliferation rather than homing, we labeled Thy1.2 6.5^+CD25^+ cells with CFSE before adoptive transfer. A control group received CFSE-labeled naive 6.5^+CD25^- cells. Animals were immunized as described before, and the phenotype of donor-derived cells in the draining lymph nodes was followed in a kinetic fashion by gating on $CD4^+Thy1.2^+$ cells. As early as 66 h after immunization, the majority of donor-derived cells in the draining lymph nodes of both groups of animals had cycled more than four times (Fig. 4). The progeny of 6.5^+CD25^+ cells had further up-regulated CD25, and CD25 was also expressed by the progeny of naive cells at this point in time, as expected. Eighty hours after immunization, cells in both groups of animals had undergone further divisions, the exact numbers of division no longer being discernable. The progeny of 6.5^+CD25^+ as well as of 6.5^+CD25^- cells appeared to divide in a "synchronized" wave (Fig. 4), probably indicating that the immunization protocol induced a transient window of productive antigen presentation in the draining lymph node. Donor-derived cells in the draining lymph nodes of both types of recipients had lost their CFSE-label 140 h after immunization. The progeny of 6.5^+CD25^+ cells contained cells that had returned to initial levels of CD25 expression, whereas others maintained elevated levels. By contrast, the progeny of naive $CD25^-$ cells had mostly lost expression of CD25. Both findings were in accord with our previous observation (compare with Fig. 3).

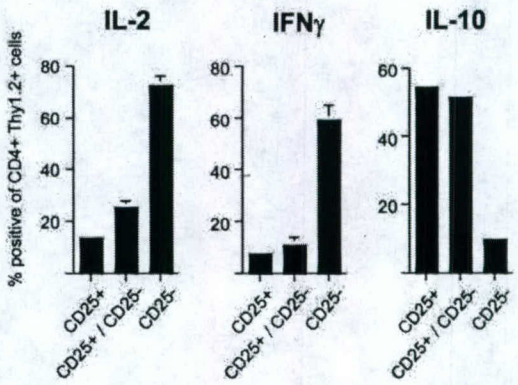

Fig. 5. Cytokine production of transferred $CD4^+CD25^+6.5^+$ T cells or $CD4^+CD25^-6.5^+$ T cells. (*a*) Transferred into Thy1.2 recipients were 3×10^5 $CD4^+CD25^+6.5^+$ T cells, $CD4^+CD25^-6.5^+$ T cells, or both. Mice were immunized with HA-peptide in IFA, and draining lymph node cells were harvested 8 days after immunization. Cells were restimulated *in vitro* with phorbol 12-myristate 13-acetate/ionomycin for 6 h in the presence of brefeldin A before surface staining for CD4 and Thy1.2, fixation, and intracellular staining for the indicated cytokine. The frequencies of cytokine-positive cells among gated $CD4^+Thy1.2^+$ draining lymph node cells of the indicated groups of animals are shown (for original data see Fig. 10).

We next performed cotransfer experiments with regulatory and CFSE-labeled naive T cells (Fig. 4 *Right*). No major difference in the early (66-h) pattern of division was observed as compared with transfer of naive cells alone. Later, when the CFSE label was lost, it was again obvious that the progeny of regulatory cells, as identified by the $CD25^+$ or $CD25^{++}$ phenotype, represented the predominant donor-derived cell type in the draining lymph node (Fig. 4, compare with Fig. 3).

Inverse Cytokine Profile of Expanded Regulators and Activated Naive CD4 T Cells. The production of cytokines by HA-specific CD4 T cells under the different conditions was tested. Three groups of Thy1.1 animals were injected with $Thy1.2^+6.5^+CD25^+$ T cells, $Thy1.2^+6.5^+CD25^-$ naive T cells, or both, and animals were immunized as described before. Eight days later, cytokine production by donor-derived cells was determined after brief restimulation *in vitro*. In recipients of 6.5^+CD25^- naive cells only, a large fraction (>60%) of $Thy1.2^+$ cells produced IL-2 and IFN-γ, whereas among the progeny of 6.5^+CD25^+ cells (expanded regulators) only few cells produced either cytokine (Fig. 5 and Fig. 10, which is published as supporting information on the PNAS web site). By contrast, a high proportion of cells produced IL-10. Among cells derived from mice that had received equal numbers of regulatory and naive HA-specific CD4 T cells, the cytokine profile closely resembled that seen in recipients of regulatory T cells alone, again suggesting that the regulatory T cells dominated the response after the 8-day period.

Regulatory $CD25^+$ T Cells Suppress the Late Expansion of Naive CD4 T Cells. To visualize more conclusively the influence of regulatory T cells on naive cells at different phases, we adoptively transferred CFSE-labeled $Thy1.1^+6.5^+CD25^-$ T cells into Thy1.2 recipients that had either received $Thy1.2^+6.5^+CD25^+$ regulatory T cells or not. Gating on $Thy1.1^+$ CD4 T cells then was used to analyze the expansion of the naive T cells after immunization. The initial recruitment of cells into the response, their proliferation rate, and the early expansion up to 90 h after the immunization were almost identical in both groups (Fig. 6 *a* and *b*, compare with Fig. 4). At 90 h after immunization, however, a plateau in the number of $Thy1.1^+$ cells among CD4 T cells was

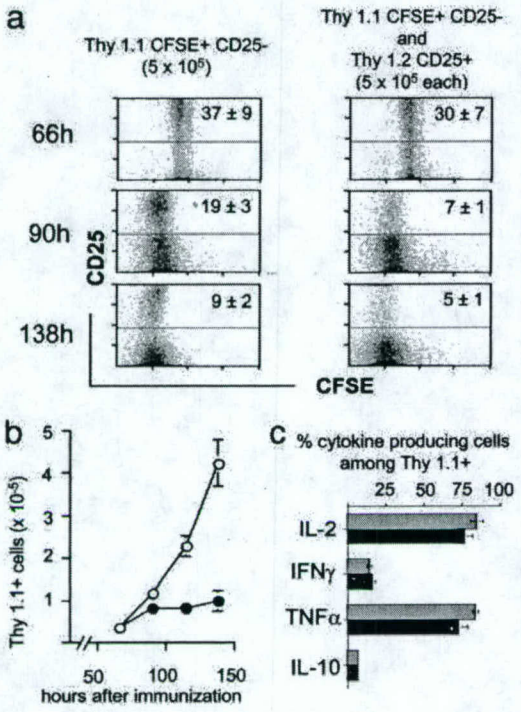

Fig. 6. Expansion, CD25 expression, and cytokine production after immunization of adoptively transferred naive $CD4^+CD25^-6.5^+$ T cells in the presence or absence of $CD4^+CD25^+6.5^+$ regulatory T cells. CFSE-labeled naive $CD4^+CD25^-6.5^+$ T cells (5×10^5) sorted from $Thy1.1^+$ *TCR-HA* mice ($rag^{+/+}$) were adoptively transferred into BALB/c Thy1.2 recipients (*Left*) or BALB/c Thy1.2 recipients that had in addition received an equal number of $CD4^+CD25^+6.5^+$ T cells from $Thy1.2^+$ *pgk-HA* × *TCR-HA* mice (*Right*). Mice were immunized as described before, and draining lymph node cells were harvested at the indicated time points after immunization. (*a*) Expression of CD25 versus CFSE fluorescence intensity on gated ($CD4^+Thy1.1^+$) progeny of naive $CD4^+CD25^-6.5^+$ T cells. Numbers within the upper quadrants indicate the frequency of $CD25^+$ cells among $CD4^+Thy1.1^+$ cells (mean of four per group). Note the "smearing" into lower-division numbers in the presence of regulatory T cells (*Right*). (*b*) Absolute number in the draining lymph nodes of the progeny of naive $CD4^+CD25^-6.5^+$ T cells after immunization in the presence (filled circles) or absence (open circles) of $CD4^+CD25^+6.5^+$ regulatory T cells (mean of four per group). The number at 0 h (i.e., without immunization) was $<0.1 \times 10^5$. (*c*) Draining lymph node cells were harvested on day 8 after immunization, stimulated *in vitro* with phorbol 12-myristate 13-acetate/ionomycin for 6 h in the presence of brefeldin A, and stained for CD4, Thy1.1, and the respective cytokine as indicated. The frequency of cytokine-producing cells among gated $Thy1.1^+CD4^+$ T cells is shown. Gray bars, recipients of naive $CD4^+CD25^-6.5^+$ T cells alone; black bars, recipients of naive $CD4^+CD25^-6.5^+$ T cells plus $CD4^+CD25^+6.5^+$ regulatory T cells (mean of four per group). TNFα, tumor necrosis factor α.

reached in animals that had received regulatory T cells (Fig. 6*b*). In contrast, in the absence of regulatory T cells the progeny of naive cells further expanded. Notably, even in the presence of regulatory T cells the majority of $Thy1.1^+$ cells continued to cycle between 90 and 138 h (Fig. 6*a*), although their number did not increase any further. Also, in the presence of regulatory T cells, a small yet distinct fraction of cells appeared to fall behind the bulk of dividing cells, discernable as a "smear" into higher CFSE intensities. Interestingly, at all time points analyzed, the fraction of cells among the progeny of naive cells expressing CD25 was lower in the presence of regulatory T cells (Fig. 6*a*).

We determined the cytokine production 8 days after immunization by $Thy1.1^+$ CD4 T cells from the two groups of mice, i.e., in either normally expanded or "suppressed" progeny of naive $CD25^-$ cells (Fig. 6*c*). The fraction of producers of IL-2, IL-10, IFN-γ, or tumor necrosis factor α was not affected significantly by suppression of their expansion through the presence of regulatory T cells, which indicated that indeed dominant expansion of regulatory T cells rather than "immune deviation" was the explanation for the observations depicted in Fig. 5.

Discussion

Most of our current understanding of the biology of suppressor T cells is derived from lymphopenic *in vivo* models or has been derived from the standard *in vitro* assay. Both types of systems have inherent limitations because of the abnormal behavior of lymphocytes in a lymphopenic environment (sometimes incorrectly referred to as homeostatic proliferation) and the questionable significance of *in vitro* observations in general. Our aim was to establish a model in which the behavior of antigen-specific $CD4^+CD25^+$ regulatory T cells and their influence on naive T cells after antigenic stimulation could be visualized *in vivo* in the context of an unperturbed immune system.

Within the time frame analyzed, the phenotype and function of $6.5^+CD25^+CD4^+$ T cells was stable after transfer into an antigen-free host. After immunization, $6.5^+CD4^+CD25^+$ T cells, despite their anergy *in vitro*, accumulated in the draining lymph nodes very much like naive T cells. CFSE labeling demonstrated that this accumulation was due to proliferation rather than preferential retention at the antigen-exposed site. These data are different from observations made with $CD25^+$ and $CD25^-$ regulatory T cells from mice that express high levels of antigen on hematopoietic cells (6), where persistent exposure to antigen may render regulatory T cells incapable of *in vivo* proliferation.

When reisolated, expanded regulators were anergic and exhibited an enhanced suppressive capacity *in vitro*, reminiscent of data showing that polyclonal $CD4^+CD25^+$ T cells after IL-2-mediated expansion *in vitro* displayed an augmented suppressive potency (22, 23). Along the same line, it had been shown that, after transfer into IL-2 receptor $\beta^{-/-}$ mice (16) or $rag^{-/-}$ mice (17), polyclonal $CD4^+CD25^+$ T cells expand *in vivo* and retain their *in vitro* suppressive properties. In the latter studies, however, it was not clear whether expansion was driven by homeostatic rather than antigen-specific mechanisms.

Can our observations *in vivo* be reconciled with current hypotheses on the action of regulatory T cells based on *in vitro* data? Generally accepted hallmarks of inhibition by $CD4^+CD25^+$ T cells *in vitro* are that (*i*) these cells are anergic, (*ii*) anergy and suppression can be broken by the addition of high amounts of exogenous IL-2, and (*iii*) inhibition is contact-dependent (reviewed in refs. 3 and 8). We consider it likely that a yet-to-be-defined milieu *in vivo*, only one component of which may or may not be IL-2, would allow for the antigen-driven proliferation of $CD4^+CD25^+$ T cells. It is not clear at present whether similarly high quantities of IL-2 as used *in vitro* are available in particular microenvironments *in vivo*. The cotransfer data presented here indicate a somewhat unexpected dynamics of suppression *in vivo* in that the regulators "outgrew" the progeny of $CD25^-$ cells, which demonstrates that proliferation and suppressive function of regulatory T cells are not mutually exclusive *in vivo*.

It has been suggested that immune regulation may act at least in part through competition for growth factors and space (24, 25). $CD25^+$ regulatory T cells, which produce IL-2 only poorly or not at all, may use IL-2 and other growth factors produced by neighboring cells for their own expansion and thus deplete these factors in the local microenvironment. We found that during their expansion, $6.5^+CD4^+CD25^+$ T cells further up-regulated CD25, which should allow for a very efficient consumption of IL-2. By contrast, the presence of regulatory T cells negatively affected CD25 expression on progeny of naive T cells. This reduction in CD25 expression may indicate IL-2 "starvation,"

THE JOURNAL OF GENE MEDICINE
J Gene Med 2004; **6**: 32–42.
Published online in Wiley InterScience (www.interscience.wiley.com). **DOI:** 10.1002/jgm.442

RESEARCH ARTICLE

Gene transfer and genetic modification of embryonic stem cells by Cre- and Cre-PR-expressing MESV-based retroviral vectors

Stelios Psarras[1†]
Niki Karagianni[1]
Christoph Kellendonk[3]
François Tronche[3]
François-Loic Cosset[4]
Carol Stocking[5]
Volker Schirrmacher[2]
Harald von Boehmer[1,6]
Khashayarsha Khazaie[1,6*]

[1]*INSERM U373, Institut Necker, Paris, France;* [2]*Division of Cellular Immunology, Tumor Immunology Program, German Cancer Research Center, Heidelberg, Germany;* [3]*Molecular Biology of the Cell I, German Cancer Research Center, Heidelberg, Germany;* [4]*Laboratory of Retroviral Vectorology and Gene Therapy, INSERM U412, Lyon, France;* [5]*Division for Cellular and Viral Genetics, Heinrich Pette Institute for Experimental Virology and Immunology, University of Hamburg, Germany;* [6]*Department of Cancer Immunology and Aids, Dana Farber Cancer Institute, Boston, USA*

*Correspondence to: Khashayarsha Khazaie, Department of Cancer Immunology and Aids, Dana Farber Cancer Institute, Smith Building 7th Floor, 44 Binney St., Boston, MA 02115, USA. E-mail: Khashayarsha_Khazaie@dfci.harvard.edu

†Present address: Allergy Unit, 2nd Pediatric Clinic, University of Athens, Greece.

Received: 19 March 2002
Revised: 23 April 2003
Accepted: 26 May 2003

Abstract

Background Genetic modification of embryonic stem (ES) cells represents a powerful tool for transgenic and developmental experiments. We report that retroviral constructs based on murine embryonal stem cell virus (MESV) can efficiently deliver and express Cre recombinase or a post-translationally inducible Cre-Progesterone receptor (Cre.PR) fusion in mouse fibroblasts and ES cells.

Methods To study the vectors a sensitive reporter cell line, 3TZ, was derived from the murine 3T6 fibroblast line that expresses β-galactosidase only upon Cre-mediated recombination. This was used together with the ROSA26-R ES cell Cre-reporter system or unmodified mouse ES cells as targets of infection. Efficiency of gene transfer was evaluated immunohistochemically by the use of an anti-Cre polyclonal antibody, and by monitoring the expression of β-galactosidase.

Results Infection of the 3TZ cells with high titer 718C or 719CP virus revealed efficient gene transduction of constitutive or hormone-inducible recombinase activity, respectively. The vectors efficiently transduced murine ES cells with Cre, Cre-PR (fusion of Cre and progesterone receptor) or β-galactosidase. Cre-mediated recombination in more than 60% of ROSA26-R ES cells was achieved when infected by a VSV-G-pseudotyped MESV retrovirus at MOI of 50.

Conclusions The MESV-based retroviral systems, when combined with hormone inducible Cre, represent efficient tools for the transfer of Cre activity in ES cells. Copyright © 2004 John Wiley & Sons, Ltd.

Keywords gene transfer; ES cells; MESV retroviral vectors; adenoviral vectors; Cre recombinase; Cre.PR fusion

Introduction

Vectors based on adenoviruses or retroviruses remain the vectors of choice for gene transfer [1,2], with MoMuLV-based vectors constituting the majority of viral constructs used in gene therapy protocols up to now [3]. Such vectors are often poor in transduction of and expression in stem cells, as well as in early embryos [4–7]. In contrast to MoMuLV, the artificial murine embryonal stem cell (MESV) retrovirus can escape transcriptional blocks in undifferentiated cells [4–10]. One of the most undifferentiated experimental tools is represented by the totipotent, mouse blastocyst-derived, embryonal

stem (ES) cells [11]. Viral gene delivery to ES cells has been a great challenge because of poor infection and poor gene expression [5]. However, MESV- and HIV (lentiviral)-based vectors have been recently used for transfer of reporter protein encoding genes into ES cells with good results [12–14].

Genetic manipulation of stem cells represents an important tool in research, as well as in clinical *ex vivo* gene therapy. In combination with ES cells, the Cre/loxP system has provided a useful tool for precise genomic modifications in transgenic animals, allowing for targeted gene activation and/or inactivation strategies [15,16]. Regulation of Cre recombinase has been recently achieved by fusing Cre to modified hormone-binding domains (HBD) of steroid receptors [17–20]. In particular, progesterone, estrogen or glucocorticoid receptor HBDs containing mutations or deletions that allow the binding of synthetic hormone analogues to the HBDs, but not of the native hormones themselves, have been fused to Cre recombinase and used in numerous *in vivo* applications [21–23].

Several recent reports have documented the possibility of genetic modification of ES cells with viral vectors [8–10,12–14,24–26]. Gene transduction efficiencies have been assessed through monitoring of the expression of reporter systems or genes conferring antibiotic resistance (e.g. green fluorescent protein, neomycin phosphotransferase II gene, etc.), indicating in some instances unpredictable stability of gene expression upon differentiation of the cells [9,10,12–14]. Limited quantitative information is available on the efficiencies of gene transduction, and of comparison of retroviral versus adenoviral gene transfer. Perhaps one of the most promising aspects of viral modification of ES cells is the use of targeted recombination, which is a permanent and irreversible genetic modification.

Retroviral delivery and expression of hormone-inducible Cre in stem cells provide a powerful experimental tool. Accordingly, we have generated MESV-based vectors expressing Cre, or Cre.PR, together with a sensitive Cre-specific read-out system (3TZ murine fibroblasts), that allows the precise titration of Cre-expressing vectors. We have conducted a quantitative analysis of the ES-specific gene transfer by these vectors into mouse fibroblasts, as well as into ES cells, and, by comparing with representative MoMuLV or adenoviral vectors, we have documented the suitability of the MESV-based retroviruses in transducing and expressing in ES cells. Finally, we were able to achieve high recombination rates with these retroviruses in a functional, ES-based, Cre assay system.

Materials and methods

Cell lines

The amphotropic retroviral packaging cell line PhoenixA[31] (ΦNX-Ampho; SBR-423) was kindly provided by Dr G. Nolan (Stanford, USA). The ecotropic retroviral packaging cell line TE-FLY-E was based on the human rhabdomyosarcoma-derived TE671 cells, as previously described [27]. The cell lines mentioned above, the human embryonic kidney-derived 293 cells, the Swiss 3T6 mouse fibroblast cell line, as well as their derived clones, were grown in Dulbecco's modified Eagle's medium (DMEM) supplemented with 10% (v/v) fetal calf serum (FCS). ROSA26-R ES cells (a kind gift from Dr P. Soriano [28]) and the HM-1 mouse embryonic stem cell line [29], kindly provided by Dr T. Magin, were maintained on mouse embryonic fibroblasts as a feeder layer, in BHK-21 medium, supplemented with 15% (v/v) FCS, 1 mM sodium pyruvate, 0.1 mM 2-mercaptoethanol, 0.1 mM NEAA, as well as 1000 U/ml leukemia inhibitory factor (LIF, Gibco) to maintain the undifferentiated phenotype. Feeder cells were prepared from 12–14-day-old C57Bl6 embryos. Growth arrest was achieved by culturing the cells in the presence of 10 μg/ml mitomycin C for 3 h.

Retro- and adenoviruses

Plasmids

All retroviral vectors constructed were based on the chimeric vector p50M [7,9]. For the construction of the p718C vector, a 1.1-kb XbaI(blunted)-EcoRI fragment containing the Cre recombinase gene fused with a nuclear localization signal [30] (NLS-Cre) was cloned into the XhoI(blunted)-EcoRI sites of the parental vector. p719CP vector was constructed by insertion of a 1.9-kb XhoI-BglII fragment from plasmid pBSMcCrePR [18], containing the NLS-Cre.PR sequence, in the XhoI-BamHI sites of the parental vector. pBSMcCrePR contains an inducible fusion between the Cre gene and a mutated form (hPR891) of the hormone-binding domain (HBD; aa 641–891) of the human progesterone receptor which lacks 42 amino acids from its C-terminus. This deletion renders PR unable to bind and respond to progesterone, yet it is still able to bind and respond to the synthetic steroid RU486 [18]. p796L vector was constructed by inserting a 3.3-kb BamHI fragment containing the nls-lacZ sequences in the BamHI site of the parental vector.

The BAG vector expresses β-galactosidase in the MoMuLV context [31]. H5.010CMVlacZ, an E1-deleted Ad5 adenovirus expressing nuclear lacZ under the CMV promoter, was kindly provided by Dr Karin Jooss [32].

Packaging

For the packaging of the retroviruses we used the ecotropic TE-FLY-E packaging cell line, the amphotropic Phoenix A packaging cell line and the VSV-G pseudotyping system [27,33,34].

For the generation of ecotropic Cre-expressing viruses, TE-FLY-E cells were plated in 60-mm dishes at 7×10^3 cells/cm^2 and transfected by the calcium phosphate method [35] using 7 μg of the viral vector plasmid together with 1 μg of the pSV2-neo plasmid (Stratagene)

carrying the neomycin phosphotransferase II gene. Neomycin-resistant colonies were selected against G418 (800 μg/ml) and further expanded.

Positive clones were further checked for Cre expression by hybridization of viral RNA, isolated from supernatants of the clones, with a Cre-specific probe. Briefly, 2 ml medium without G418, conditioned for 48 h with subconfluent cultures of each individual clone grown in 25-cm^2 flasks, were collected, filtered through a 45-μm filter, incubated for 30 min at 37 °C in 10 mM EDTA, 100 μg/ml proteinase K, 0.5% (w/v) SDS, acid phenol and chloroform extracted and ethanol precipitated together with 5 μg tRNA as carrier. RNA was resuspended in 50 μl TE buffer, 75 μl formamide and 25 μl formaldehyde (37%, v/v) were added, and samples were incubated for 10 min at 60 °C. The RNA was then diluted in 10× SSC, applied in 1:3 serial dilutions to a dot blot apparatus on nitrocellulose membrane and hybridized with a Cre-specific probe according to Church and Gilbert [36].

The viral supernatants were in parallel subjected to titration of their infectious activity using the especially developed Cre-activity read-out system of 3TZ fibroblasts. Cre producer clones revealed by both methods are further referred to as TEC cells (for TE-FLY-E generated, MESV-based, Cre-expressing retrovirus). Best clones (e.g. TEC3) were further expanded and viral supernatants were collected from confluent cultures, titrated and used throughout this study.

Alternatively, TE-FLY-E cells were plated at 100, 10 or 1 cells/well in 48-well plates and infected with amphotropic virus containing supernatant produced by transient transfection of PhoenixA with p796L vector plasmid as described below. The titers of the emerging clones were estimated using 3T6 cells as read-out system and lacZ producers are further referred to as TEZ clones (for TE-FLY-E generated, MESV-based, LacZ-expressing retrovirus), unless specified otherwise.

The amphotropic viruses were produced by transiently transfecting 10 μg of each plasmid into Phoenix A cells plated in 60-mm dishes at 7×10^4 cells/cm^2 by the chloroquine/calcium phosphate method, as described [37]. Fresh medium (3 ml) was added 1 day post-transfection and collected 48 h later. Supernatants were filtered through a 45-μm filter and titers were estimated using the 3TZ read-out system (see below).

For the VSV-G pseudotyping, 293 cells were transiently transfected as described above with the pMD.gagpol and the pMDtet.G plasmids (expressing the MoMuLV gag-pol and the VSV-G protein, respectively, both kind gifts of Dr R. Mulligan [34]) together with the retroviral vector. Supernatants were collected 48 h later and were further handled as described [38].

Viral infection

3T6 or 3TZ cells were plated at 1.0×10^4 cells/cm^2; HM1 ES cells were plated at $0.35–1.0 \times 10^5$ cells/cm^2 on feeder cells (1.0×10^5 feeder cells/cm^2) in 6- or 24-well plates. Cells were infected the next day in the presence of 8 μg/ml polybrene with serial dilutions of the respective viral supernatants, representing thus different multiplicity of infection (MOI) ratios, calculated against cell numbers at the time of infection. Then, 12–16 h later, medium was changed and Cre or β-galactosidase expression was detected 2 days later by either X-Gal staining or staining with an anti-Cre antibody (see below). Viral titers (IU/ml; infectious units contained per ml of supernatant) were calculated by multiplying the numbers of transduced cells by the dilution factor of the supernatant. For the 719CP virus the term 'Cre-active particles' was used, taking into account that the numbers of cells expressing Cre activity in the absence of RU486 do not reflect the actual transduction efficiency seen in the presence of the hormone analogue, but rather the fraction of cells transduced with a leaky transgene. For adenoviral infections an identical infection protocol was followed, including the presence of polybrene, which has been shown to facilitate adenovirus-mediated gene transfer in various cell lines [39].

Transfection

3TZ cells were plated at 1.0×10^4 cells/cm^2 in 6-well plates. The next day, the cells were transfected with 5 μg of p718C or p719CP plasmid DNA using the calcium phosphate method [35]. Twenty-four hours later, cells were washed with PBS, incubated for 10 min at 37 °C with HBSS solution (Gibco) and further incubated with normal growth medium with or without 0.1 μM RU486 (Sigma, St. Louis, WI, USA). Forty-eight hours later, cells were fixed and stained with X-Gal for detection of β-galactosidase activity (see below).

Generation of a Cre activity reporter system

For the generation of the 3TZ Cre activity read-out system, 10^7 mouse 3T6 fibroblasts were suspended in 0.8 ml PBS and electroporated (BioRad gene pulser; 960 μF, 300 V) with 4 μg of the NotI-linearized pψβ-galoxé plasmid, which expresses β-galactosidase only after Cre-mediated recombination [18] (see Figure 1B). Stable clones were selected against G418 (800 μg/ml) and further expanded. Positive clones were plated in duplicates in 24-well plates at 2×10^4 cells/well and infected with Cre-expressing retroviral particles at MOI of 10 or left untreated. Forty-eight hours after infection, cells were fixed and stained with X-Gal. Only clones with the absence of any β-galactosidase activity in the untreated cultures and 100% blue-stained cells in the infected ones were further processed for Southern analysis (EcoRI digestion) performed by standard procedures.

Detection of Cre expression with anti-Cre antibody

Cells were plated on coverslips at 60–80% confluency. On the next day they were washed twice with PBS, fixed

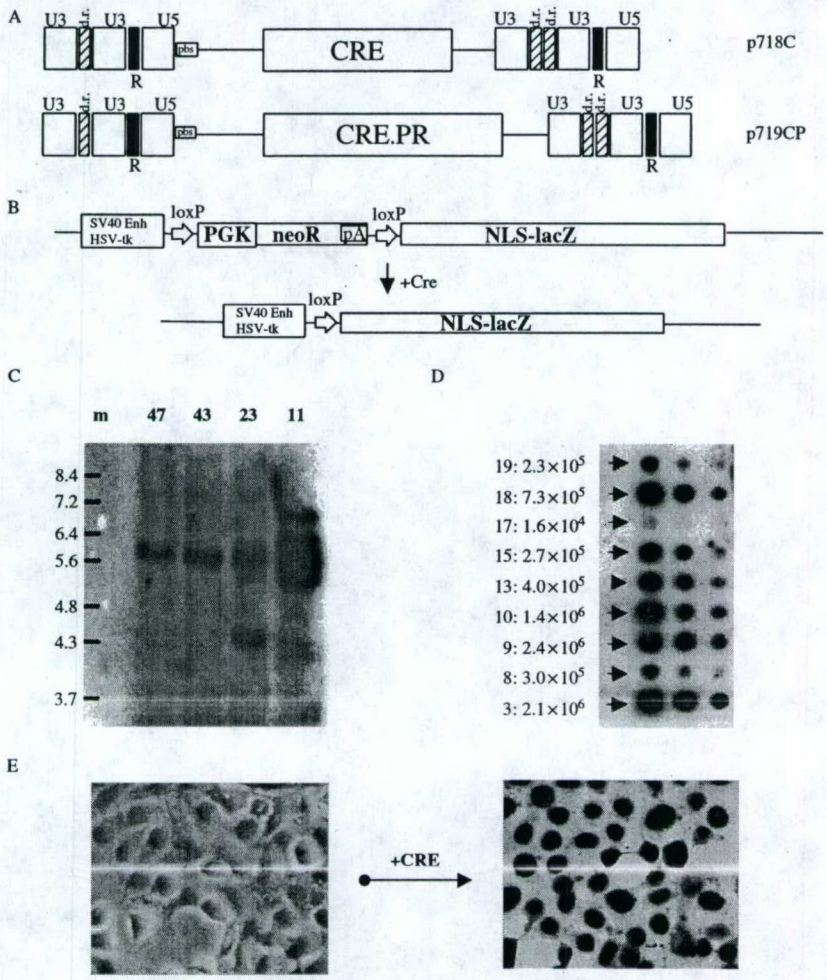

Figure 1. Generation of retroviral vectors expressing Cre recombinase. (A) Chimeric retroviral vectors expressing constitutive (p718C) or RU486-inducible (p719CP) Cre recombinase; pbs: primer binding site (here: MESV pbs for $tRNA^{glu}$); d.r.: direct repeat; U3, R, U5: regulatory elements of MoMuLV-based LTRs. The 5′ LTR, containing one characteristic direct repeat sequence in the U3 region, is from PCMV whereas the 3′ LTR, containing two direct repeats, is from MPSV. The vectors are depicted before integration. (B) Schematic representation of the construct used for the generation of the Cre-specific read-out system: Nuclear lacZ is expressed under HSV-tk promoter and SV40 enhancer elements only after a Cre-mediated loxP recombination event, which leads to the excision of the neoR unit. neoR: neomycin phosphotransferase II gene; PGK: phosphoglycerate kinase promoter; pA: SV40 polyadenylation signal. (C) Southern analysis of 3TZ clones: 3T6 cells were stably transfected with the Cre-reporter construct of (B). DNA from individual, G418-resistant clones (3TZ cells) were digested with EcoRI, and further subjected to Southern analysis using a lacZ-specific probe, to test for the integrity of the reporter construct. m: molecular weight marker in kb. (D) Packaging of the Cre retrovirus: dot blot of viral RNA (1 : 3 serial dilutions) isolated from the supernatants of nine individual clones (3, 8, 9, 10, 13, 15, 17, 18 and 19) of TE-FLY-E packaging cells stably transfected with p718C. RNA was immobilized on nitrocellulose membrane and hybridized to a ^{32}P-labelled Cre-specific probe. The titers in IU/ml were estimated using the Cre-specific 3TZ read-out system. (E) Cre-reporter functional assay: non-treated (left) or virus-infected (right) 3TZ 43 cells were fixed, stained overnight with X-Gal (1 mg/ml) staining solution and photographed. 100% of the cells of the clone 3TZ 43 express β-galactosidase in the nucleus after infection with Cre retrovirus at MOI 10, whereas the non-treated ones show absolutely no background. Original magnification ×50

for 10–15 min at room temperature (RT) with 3.7% (v/v) formaldehyde in PBS, washed three times with PBS, incubated for 5 min at RT with blocking buffer (250 mM KCl, 40 mM Hepes pH 7.9, 0.5% (w/v) BSA, 0.5% (v/v) gold fish gelatin, 0.1% (v/v) Triton X-100), incubated for 45 min at RT with 1 : 2000 dilution of a rabbit anti-Cre polyclonal antibody (PRB-106C; Covance, Princeton, NJ, USA) in blocking buffer, washed three times in blocking buffer, incubated for 45 min at RT with 1 : 100 dilution of phycoerythrin-labelled goat anti-rabbit IgG (GAR-PE, stock 1 mg/ml; Molecular Probes) in blocking buffer, washed three times in blocking buffer, once in PBS, incubated for 5 min with 4,6-diamidino-2-phenylindole (DAPI) in PBS, washed three times in PBS and placed

on microscope slides with a drop of mounting medium (Immuno Fluore; ICN). Fluorescence was detected using a Leitz DMRB fluorescence microscope.

Detection of β-galactosidase-induced expression with X-Gal staining

Cultures were washed with PBS, fixed for 10 min with 3.5% (v/v) formaldehyde, 0.5% (v/v) glutaraldehyde, washed twice with PBS and stained from 4 h to overnight in X-Gal staining solution (2 mM $MgCl_2$; 5 mM $K_3Fe(CN)_6$; 5 mM $K_4Fe(CN)_6$; 0.01% (w/v) sodium deoxycholate; 0.02% (v/v) Nonidet P-40; 1 mg/ml X-Gal). Cells expressing β-galactosidase were counted under a Leica DM IL light microscope.

Results

MESV-based retroviral vectors for Cre delivery and 3TZ read-out system for Cre activity

For the present study we constructed retroviral vectors based on the p50M chimeric vector of the MESV type, which, in contrast to its prototype MoMuLV, has been reported to express in undifferentiated cells [5,7–9]. Expression of this vector in ES cells benefits from the use of LTR sequences from MoMuLV derivatives, namely the myeloproliferative sarcoma virus (MPSV; at the 3′ LTR) and the PCC4-cell-passaged MPSV (PCMV; at the 5′ LTR, Figure 1A), as well as from the replacement of its natural tRNA binding site (pbs) by the one of the endogenous murine dl-587rev retrovirus [7–9].

Two types of vectors were generated using the p50M backbone (Figure 1A): (a) p718C: encoding the Cre recombinase gene, and (b) p719CP: encoding an inducible fusion between the Cre gene and a mutated form of the hormone-binding domain (HBD; aa 641–891) of the human progesterone receptor (Cre.PR). In the absence of ligand, Cre is inactive within the Cre.PR, due to the interaction of the HBD moiety with the steroid receptors regulatory system, whereas, upon RU486 binding, it passes to the active state.

Viral particles were generated from stable co-transfection of TE-FLY-E ecotropic packaging cells with vector and a plasmid conferring neomycin resistance, as well as transient transfection of the PhoenixA amphotropic packaging cell line. 12 out of 20 p718C transfected, neomycin-resistant clones produced retroviral particles containing the Cre gene (Figure 1D and data not shown). Comparable viral titers were obtained by transfecting the p719CP or p718C construct in the PhoenixA amphotropic packaging cell line (4.1×10^5 IU/ml; Figure 2B).

To titrate the supernatants for delivery of Cre activity, the 3T6 murine fibroblast cell line was transfected with a Cre-dependent β-galactosidase expression cassette (3TZ

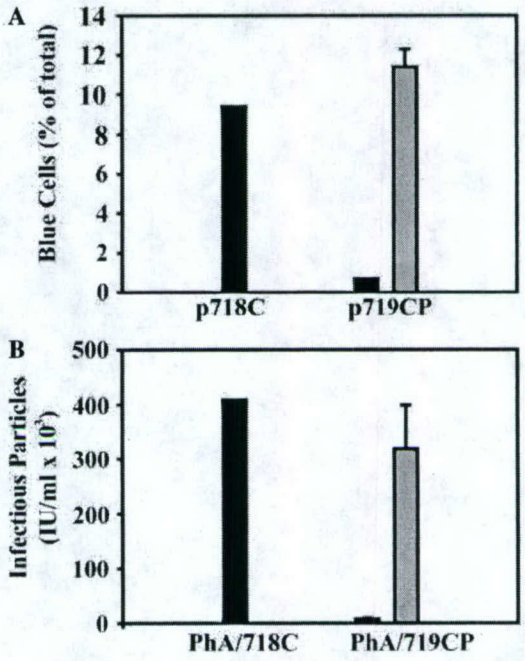

Figure 2. Inducibility of Cre.PR in the retroviral context. (A) Transfection. 3TZ cells were transfected with either p718C or p719CP using the calcium phosphate method. Cultures were further grown in the presence or absence of 0.1 μM RU486. Forty-eight hours later the percentages of total cell population which expressed β-galactosidase were calculated. Mean of two representative experiments. Grey bars: 0.1 μM RU486. Black bars: no hormone added. (B) Infection. 3TZ cells were infected in the presence of 8 μg/ml polybrene with supernatants from PhoenixA cells previously transfected with either p718C or p719CP. Cultures were grown for 48 h in the presence or absence of 0.1 μM RU486. Apparent titers in IU/ml were estimated as described in Materials and methods. Mean of three representative experiments. Grey bars: 0.1 μM RU486. Black bars: no hormone added

cells). In the Cre-dependent, β-galactosidase expression cassette, nls-lacZ is separated from an active promoter by a neomycin phosphotransferase II (neo^R) minigene (Figure 1B). Upon Cre-mediated recombination, the loxP-flanked neo^R minigene is excised and lacZ is expressed from the HSV-tk promoter and SV40 enhancer elements.

Clone 43 (3TZ43) contained only intact copy/copies of the transfected DNA (Figure 1C), which remained stable throughout extensive *in vitro* serial passaging, and showed no background of β-galactosidase in the absence of Cre. On the other hand, 100% of these cells were able to express β-galactosidase upon expression of Cre (Figure 1E and data not shown), thus avoiding contaminating, non-staining cell populations observed in similar read-outs [43], possibly resulting from tandem arrays of the integrated reporter construct [44]. The uniform nuclear β-galactosidase staining of the 3TZ 43 cells provides a highly sensitive *in vitro* assay for the detection of Cre activity expressed by both amphotropic and ecotropic retroviruses, an ability not shared by other

Cre-reporter systems based on simian [18,44,45], feline [46] or human cell lines [47].

Validation of MESV vectors and delivery of Cre activity in 3TZ cells

Using the 3TZ read-out system, the titers of supernatants, produced by several TE-FLY-E clones stably transfected with p718C (TEC cells), were estimated to range from 1.6×10^4 to 2.4×10^6 IU/ml. These results were in agreement with the intensities of the respective RNA dot blots, resulting from viral RNA hybridized with a ^{32}P-labelled Cre-specific probe (Figure 1D and data not shown). When cultured at higher cell densities the high producer TEC3 clone was able to generate viral titers up to 2.6×10^7 IU/ml, this being up to an order of magnitude higher than the titers reported for earlier vectors expressing Cre together with selectable markers [48].

Transfection and viral gene transduction were compared for delivering tight hormone-dependent regulation of Cre activity with the p719CP construct. Transient transfection of the 3TZ 43 cells line with p718C or p719CP DNA in the presence of 0.1 μM RU486 revealed comparable levels of Cre activities, with 9.4 and 11.5% of the cells staining for β-galactosidase activity, respectively. Detectable levels of hormone-independent Cre activity were observed in p719CP-transfected cells, with 0.8% of the cells expressing β-galactosidase in the absence of RU486 (Figure 2A). This corresponds to 8.5% of the total transfected cells, as estimated from the number of blue-stained cells produced by transfecting 3TZ cells with the p718C. Leaky Cre.PR activity was reduced to 2.4% of total transfected cells upon viral gene transduction. This allowed for a more pronounced relative induction of Cre activity in the presence of RU486 in virally transduced cells (average: 40.8-fold), as compared with transfected cells (average: 15.5-fold). These results demonstrate tight RU486-dependent regulation of Cre.PR activity in retrovirally transduced cells.

Comparison with Moloney retroviral and adenoviral vectors expressing constitutively active LacZ in ES cells

In order to directly quantitate the MESV-mediated gene transduction into ES cells, the p796L retrovirus encoding *E. coli* LacZ was constructed using the same retroviral vector backbone as the p718C virus (Figure 4A). Infectious particles were generated using the TE-FLY-E packaging cell line, and stable clones (TEZ) were isolated that produced viral titers of up to 0.9×10^7 IU/ml. To compare efficiencies of amphotropic and ecotropic env in mediating infection of ES cells, the p796L virus was also packaged transiently using the PhoenixA cell line (PhA/796L) and equal numbers of viral particles as assayed on 3T6 cells were used to infect HM1 ES cells. Infection of HM1 ES cells by TEZ/796L or PhA/796L retrovirus particles revealed comparable gene transduction efficiencies of 5.3 ± 0.4 and $5.05 \pm 0.15\%$, as compared with infection of 3T6 cells, respectively (Figure 4C), indicating that both ecotropic and amphotropic pseudotyping are suitable for this purpose.

The relative transduction efficiency was unchanged ($5.55 \pm 0.85\%$) when 20 times more TEZ/796L packaged viral particles were used (Figure 4B). In contrast, infections by the BAG retroviral vector (MoMuLV-based retrovirus encoding lacZ) [31] packaged in PhoenixA cells (PhA/BAG virus) resulted in the transduction of only $0.06 \pm 0.035\%$ of the ES cells, as compared to fibroblasts. These results are in agreement with MESV being significantly more efficient than MoMLV in transducing ES cells.

We next compared the 796L retrovirus to an adenoviral vector expressing β-galactosidase under the cytomegalovirus (CMV) immediate early promoter (H5.010CMVlacZ [32], referred to here as AdlacZ). By conducting a series of infections at a variety of MOIs (ranging from 1:17 to 14:1) we observed that both viruses were able to transduce β-galactosidase activity into HM1 ES cells, with the absolute numbers of β-galactosidase-expressing ES cells ('blue' cells) increasing as the quantities of added fibroblast active viral particles increased (data not shown), this being at variance with a previous work reporting the failure of a similar AdlacZ virus to transduce undifferentiated ES cells [26]. However, AdlacZ transduced preferentially the mouse embryonic fibroblasts (MEFs) used as feeders for the HM1 ES cells (Figures 4E and 4G). By averaging the results of several experiments conducted at different MOIs (ranging from 1:7–14:1), it was estimated that 53.15% (±4.35) of the total X-Gal-stained cells per culture, after AdlacZ treatment, were morphologically MEF feeder cells (Figures 4D and 4F). This result is even more striking when considering that the MEFs represented only 11–16% of the total mixed ES and MEF cell population.

MESV-based vectors can efficiently deliver Cre to ES cells, and promote Cre-mediated recombination in ROSA ES cells

The ability of p718C to transduce Cre recombinase into ES cells was tested using a polyclonal antibody against Cre. This antibody was able to detect Cre recombinase in TE-FLY-E cells stably transfected with p718C (TEC clones). In particular, immunohistochemical staining of the high-producer TEC3 clone revealed the presence of nuclear localized Cre in 100% of the cells, whereas untransfected TE-FLY-E cells did not stain (Figure 3B and data not shown). Similarly, HM1 ES cells previously infected with TEC3 supernatants were specifically stained by the Cre antibody, indicating that the MESV-based p718C retroviral vector efficiently transfers Cre recombinase in ES cells (Figure 3D and data not shown).

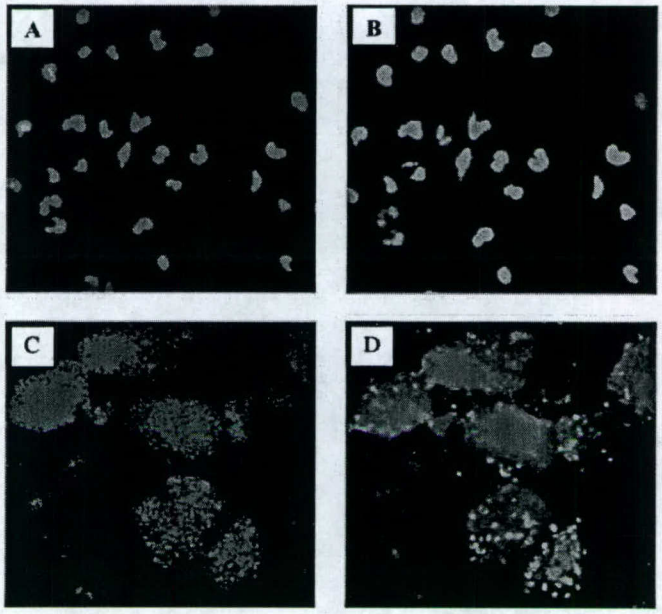

Figure 3.

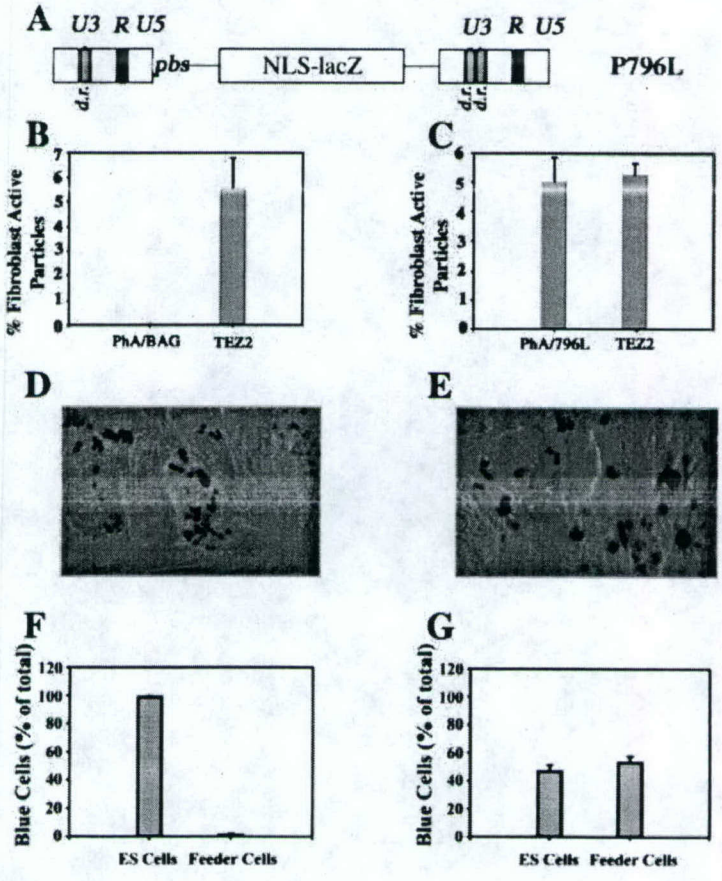

Figure 4.

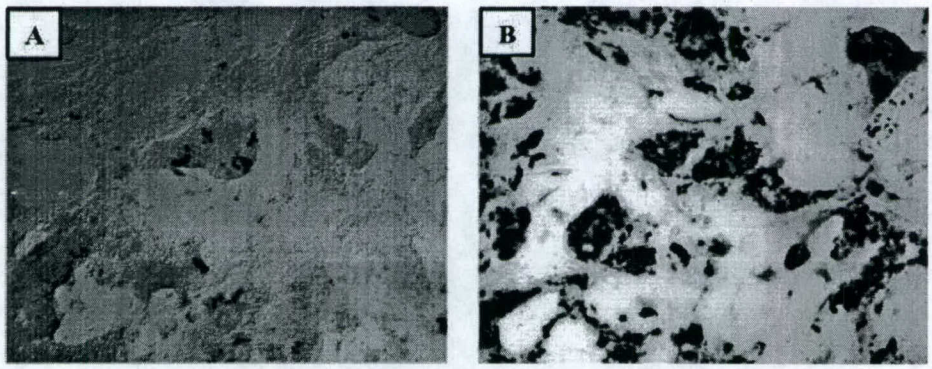

Figure 5. High efficiency MESV-mediated transfer of Cre recombinase to ES cells. ROSA26-R ES cells were plated at 10^4 cells/cm^2 in 6-well plates on feeder fibroblasts. One day later they were infected with VSV-G-pseudotyped Cre retrovirus at MOI 0.5 (A) or 50 (B) in the presence of 8 μg/ml polybrene. Two days later cells were fixed, stained overnight with X-Gal (1 mg/ml) staining solution and photographed. Original magnification ×100

To test the ability of this retroviral system to transfer Cre activity in ES cells, we used the ROSA26-R ES cell read-out system, and VSV-G pseudotyped virus, which allows pelleting of the virus by ultracentrifugation and virus concentration without loss of activity [38]. Up to 20 times higher titers were achieved by this method, reaching 5×10^8 3TZ infectious units per ml. Using high titer virus, at MOI 50, functional recombination was achieved in the majority of ES cells (Figure 5B). At MOI 0.5, $1.54 \pm 0.71\%$ of the population, and, at MOI 0.005, $0.21 \pm 0.02\%$ of ES cells were transduced, suggesting that transduction of ES cells by the VSV-G-pseudotyped virus is disproportionate to the input of Cre-expressing viral particles, as was also the case for the MoMuLV-enveloped virus (not shown).

Discussion

The goal of the present work was to generate and analyze viral vectors that efficiently express Cre and hormone-inducible Cre in embryonic stem cells. Viral titers were compared using a novel Cre-reporter system based on 3T6 fibroblasts, which we showed are also susceptible to infection with adenoviral vectors. Similar read-out systems derived from NIH-3T3 [40] have been reported, which are likely to lack adenovirus receptors [41,42].

Our finding that retroviral transduction of mouse fibroblasts with p719CP allows for tighter regulation of the expressing Cre.PR by RU486, as compared with transfection techniques, is of importance for the transfer of this and other post-translationally controlled Cre systems in cells. The higher leakiness observed upon transfection of the vector DNA may be due to several reasons: (1) The stress of transfection may transiently interfere with the mechanism of regulation of the steroid receptors. (2) Large quantities of DNA taken up by the cells may lead to high levels of expression of Cre.PR, thus overwhelming the natural regulation of steroid

Figure 3. Detection of Cre recombinase in ES cells infected with TEC3 supernatants. (A, B) TEC3 cells were plated on glass coverslips at 1.0×10^4 cells/cm^2. Next day they were immunostained with a rabbit anti-Cre polyclonal antibody. Nuclei stained with DAPI were identified under UV light (A), whereas nuclear localized Cre could be visualized after staining with a phycoerythrin-labelled secondary antibody (B). Original magnification ×40. (C, D) HM1 ES cells were plated on glass coverslips at 0.5×10^5 cells/cm^2. The next day they were infected with TEC3 supernatants in the presence of 8 μg/ml polybrene. Two days later cells expressing Cre were immunostained with a rabbit anti-Cre polyclonal antibody followed by a phycoerythrin-labelled secondary antibody (D). Nuclei were visualized using DAPI staining (C). Original magnification ×20

Figure 4. Differential pattern of infection of HM1 ES cells by 796L and AdlacZ viruses. (A) MESV-based retroviral vector expressing *E. coli* β-galactosidase containing a nuclear location signal (p796L); pbs: primer binding site (here: MESV pbs for $tRNA^{glu}$); d.r.: direct repeat; U3, R, U5: regulatory elements of MoMuLV-based LTRs. (B) HM1 ES cells were plated on feeder cells. The next day they were infected in the presence of 8 μg/ml polybrene with 1×10^4 'fibroblast-active particles' of either PhA/BAG or TEZ2/p796L virus. Two days later cells were fixed and stained with X-Gal staining solution. Numbers of blue cells were expressed as percentages of the input fibroblast-active particles. Mean of three independent experiments. (C) HM1 ES cells were plated on feeder cells. The next day they were infected in the presence of 8 μg/ml polybrene with 2.5×10^5 'fibroblast-active' particles of either PhA/796L or TEZ2/p796L virus. Two days later cells were fixed and stained with X-Gal staining solution. Numbers of blue cells were expressed as percentages of the input fibroblast-active particles. Mean of two independent experiments. (D, E) HM1 ES cells were plated at 0.35×10^5 cells/cm^2 on feeder cells (previously plated at 1.0×10^5 cells/cm^2). The next day they were infected in the presence of 8 μg/ml polybrene with 5×10^5 'fibroblast-active' particles of either TEZ2 (D) or AdlacZ virus (E). Two days later cells were fixed and stained with X-Gal staining solution. Original magnifications ×50. (F, G) Percentages of total X-Gal-stained cells identified as blue-stained ES cells and blue-stained feeder cells, respectively. Mean of two representative retroviral TEZ2 infections (F) and eight adenoviral AdlacZ infections (G)

receptors [53]. (3) Mutations, rearrangements or partial degradation of DNA taken up by the transfected cells may inactivate or delete the PR domain in a fraction of the expressed proviral DNA. In contrast to DNA transfection, retroviral gene transduction characteristically leads to the integration of only a limited number of intact functional copies, with minimal stress for the target cells.

Retroviral vectors transduce ES cells considerably less efficiently than fibroblasts [10,12]. Similar results were obtained even when transgene expression was driven from internal promoters theoretically avoiding the LTR-mediated transcriptional silencing in ES cells [25]. On the other hand, Laker *et al.* [9], measuring neo resistance conferred from monocistronic MESV vectors, reported comparable efficiencies of gene transduction for either ES cells or NIH3T3 fibroblasts, whereas bicistronic vectors preferentially transduced the fibroblasts. Variations in the relative efficiencies of transduction into ES cells could in part be attributed to the different titration methods used, to differences in construct characteristics such as splicing signals and number of cistrons included, or to the different ES cell lines used [8].

The poor gene expression afforded by MoMuLV-derived vectors in embryonic carcinoma (EC) and ES cells [5] is partially circumvented by MESV-based [8–10] or MND [10] vectors. We were able to show that the MESV-based retrovirus can transfer Cre activity into ES cells. This was shown both by immunostaining documenting the presence of Cre protein in the target cells, as well as by assessing its recombinogenic activity in a functional ES cell assay. The latter system allowed us to achieve high (over 60%) transduction efficiencies.

By infecting with equal quantities of retroviral particles, estimated from transduction of mouse fibroblasts, we were able to calculate that MESV-based vectors can transduce the ES cells approximately by two orders of magnitude more efficiently than vectors containing original MoMuLV LTRs and pbs. This improvement is substantially stronger than that observed by Robbins *et al.* [10] who, using a MoMuLV-based vector expressing the chloramphenicol acetyltransferase (CAT) gene, estimated a 12% relative CAT activity in CCE ES cells compared with PA317 fibroblasts and only a 4-fold improvement with the use of the MESV-like, MND vector. Others have reported failure of MoMLV-driven transgene expression in ES cells [12].

Our findings are consistent with results recently reported for transduction of fluorescent markers into ES cells using retroviral vectors [12–14]. It should be noted, however, that efficiencies reported here have been achieved in some cases only when exposing the cells to extremely high excess of viral particles (e.g. at MOI nearly 600 [13]), whereas in other systems more modest conditions are required [14]. Insertion of regulatory elements such as the woodchuck hepatitis B virus post-transcriptional regulatory element or VSV-G pseudotyping was reported to increase efficiency of transduction to levels comparable to those mediated by lentiviral vectors [13,14].

Comparison of 796L with AdlacZ-mediated gene transfer into ES cells revealed that the retroviral vector preferentially transduced ES cells, as compared with the AdlacZ vector that transduced preferentially the MEFs used as feeders in the ES culture. The preferential infection of MEFs could potentially be related to the fact that the MEFs were mitotically blocked by mitomycin treatment [49] as well as to a relative abundance of the main adenovirus receptor, the CAR receptor [42], in MEFs as compared to ES cells. Variable expression of this receptor has been recently shown for other cell lines [50,51]. By analogy, the relative failure of adenoviral vectors to transduce another type of stem cell, the hematopoietic stem cell, has been attributed to low or undetectable adenovirus receptor levels [52]. It should also be noted that our relative efficiency of ES transduction by AdlacZ (as compared with the transduction of fibroblasts infected by the same vector) was significantly lower than the 30–50% efficiency reported for the infection of AB1 ES cells at the high MOI of 100, with an adenoviral vector expressing neo^R under the PGK promoter [24]. One reason for this may be more efficient activity of the PGK promoter as compared with that of the CMV promoter in ES cells. However, the estimations in that report were deduced from Southern blot analysis, essentially differing from our assay. Nevertheless, the CMV promoter is the most commonly used internal promoter in adenoviral vectors in numerous *in vivo* applications [3].

Transgene expression from retrovirally modified ES cells is silenced in the emerging mice through both methylation-dependent and -independent mechanisms, even when the retrovirus used is of the MESV-type [12]. Accordingly, this transcriptional repression can be partially circumvented by the use of 5-azadeoxycytidine. MESV-driven transgene expression was reported to be maintained upon differentiation of ES cells or hematopoietic progenitor cells [12], allowing the use of retrovirally modified stem cells for developmental experiments, as a viable alternative to the recently established lentivirus-based systems [13]. Transfer and activation of Cre in appropriately modified stem cells allow for irreversible site-directed mutagenesis, which in any case does not suffer from shut down of retroviral gene expression afterwards. The post-translational regulation of Cre-mediated recombination in ES cells also limits the timing, extent and the potential toxic effects of Cre activity [54]. The fact that Cre.PR can be efficiently activated in the presence of RU486 in murine ES cells [18] renders this regulatory system a powerful tool for inducible site-specific recombination in embryonic and other stem cells.

In summary, using the Cre- or Cre.PR-expressing p718C and p719CP retroviruses we were able to achieve efficient gene transduction and high Cre/loxP recombination rates in two different ES cell lines. These studies indicate that the MESV-based retroviral vectors are suitable vectors for gene transfer and genetic modification of ES cells.

Acknowledgements

We wish to thank Dr Karin Jooss for generously providing us with purified AdlacZ, Sylvie Chapel-Fernandez for the generation of TE-FLY-E cells, and also Annette Lichtenauer for excellent technical assistance. S.P. was a recipient of a Schering Research Foundation fellowship (Berlin). N.K. was supported by an IARC research fellowship. This work was in part supported by the Department of the Army, Breast Cancer Research Idea Award DAMD17-02-1-0361 (KK).

References

1. Reynolds PN, Feng M, Curiel DT. Chimeric viral vectors – the best of both worlds? *Mol Med Today* 1999; **5**: 25–31.
2. Kay MA, Glorioso JC, Naldini L. Viral vectors for gene therapy: the art of turning infectious agents into vehicles of therapeutics. *Nat Med* 2001; **7**: 33–40.
3. Mountain A. Gene therapy: the first decade. *Trends Biotechnol* 2000; **18**: 119–128.
4. Stewart CL, Schuetze S, Vanek M, Wagner EF. Expression of retroviral vectors in transgenic mice obtained by embryo infection. *Embo J* 1987; **6**: 383–388.
5. Stocking CG, Ma OW. *Regulation of Retrovirus Infection and Expression in Embryonic and Hematopoietic Stem Cells*. Doerfler W, Bohm P (eds). VCH: Weinheim, 1993; 433–455.
6. Robbins PB, Skelton DC, Yu XJ, Halene S, Leonard EH, Kohn DB. Consistent, persistent expression from modified retroviral vectors in murine hematopoietic stem cells. *Proc Natl Acad Sci U S A* 1998; **95**: 10 182–10 187.
7. Baum C, Hegewisch-Becker S, Eckert HG, Stocking C, Ostertag W. Novel retroviral vectors for efficient expression of the multidrug resistance (mdr-1) gene in early hematopoietic cells. *J Virol* 1995; **69**: 7541–7547.
8. Grez M, Akgun E, Hilberg F, Ostertag W. Embryonic stem cell virus, a recombinant murine retrovirus with expression in embryonic stem cells. *Proc Natl Acad Sci U S A* 1990; **87**: 9202–9206.
9. Laker C, Meyer J, Schopen A, *et al*. Host cis-mediated extinction of a retrovirus permissive for expression in embryonal stem cells during differentiation. *J Virol* 1998; **72**: 339–348.
10. Robbins PB, Yu XJ, Skelton DM, *et al*. Increased probability of expression from modified retroviral vectors in embryonal stem cells and embryonal carcinoma cells. *J Virol* 1997; **71**: 9466–9474.
11. Weissman IL. Translating stem and progenitor cell biology to the clinic: barriers and opportunities. *Science* 2000; **287**: 1442–1446.
12. Cherry SR, Biniszkiewicz D, van_Parijs L, Baltimore D, Jaenisch R. Retroviral expression in embryonic stem cells and hematopoietic stem cells. *Mol Cell Biol* 2000; **20**: 7419–7426.
13. Hamaguchi I, Woods NB, Panagopoulos I, *et al*. Lentivirus vector gene expression during ES cell-derived hematopoietic development in vitro. *J Virol* 2000; **74**: 10 778–10 784.
14. Ketteler R, Glaser S, Sandra O, Martens UM, Klingmuller U. Enhanced transgene expression in primitive hematopoietic progenitor cells and embryonic stem cells efficiently transduced by optimized retroviral hybrid vectors. *Gene Ther* 2002; **9**: 477–487.
15. Rajewsky K, Gu H, Kuhn R, *et al*. Conditional gene targeting. *J Clin Invest* 1996; **98**: 600–603.
16. Rossant J, McMahon A. "Cre"-ating mouse mutants – a meeting review on conditional mouse genetics. *Genes Develop* 1999; **13**: 142–145.
17. Zhang Y, Riesterer C, Ayrall AM, Sablitzky F, Littlewood TD, Reth M. Inducible site-directed recombination in mouse embryonic stem cells. *Nucleic Acids Res* 1996; **24**: 543–548.
18. Kellendonk C, Tronche F, Monaghan AP, Angrand PO, Stewart F, Schutz G. Regulation of Cre recombinase activity by the synthetic steroid RU 486. *Nucleic Acids Res* 1996; **24**: 1404–1411.
19. Feil R, Wagner J, Metzger D, Chambon P. Regulation of Cre recombinase activity by mutated estrogen receptor ligand-binding domains. *Biochem Biophys Res Commun* 1997; **237**: 752–757.
20. Brocard J, Feil R, Chambon P, Metzger D. A chimeric Cre recombinase inducible by synthetic, but not by natural ligands of the glucocorticoid receptor. *Nucleic Acids Res* 1998; **26**: 4086–4090.
21. Brocard J, Warot X, Wendling O, *et al*. Spatio-temporally controlled site-specific somatic mutagenesis in the mouse. *Proc Natl Acad Sci U S A* 1997; **94**: 14 559–14 563.
22. Schwenk F, Kuhn R, Angrand PO, Rajewsky K, Stewart AF. Temporally and spatially regulated somatic mutagenesis in mice. *Nucleic Acids Res* 1998; **26**: 1427–1432.
23. Kellendonk C, Tronche F, Casanova E, Anlag K, Opherk C, Schutz G. Inducible site-specific recombination in the brain. *J Mol Biol* 1999; **285**: 175–182.
24. Mitani K, Wakamiya M, Hasty P, Graham FL, Bradley A, Caskey CT. Gene targeting in mouse embryonic stem cells with an adenoviral vector. *Somatic Cell Mol Genet* 1995; **21**: 221–231.
25. Soriano P, Friedrich G, Lawinger P. Promoter interactions in retrovirus vectors introduced into fibroblasts and embryonic stem cells. *J Virol* 1991; **65**: 2314–2319.
26. Rust EM, Westfall MV, Samuelson LC, Metzger JM. Gene transfer into mouse embryonic stem cell-derived cardiac myocytes mediated by recombinant adenovirus. *In Vitro Cell Develop Biol Anim* 1997; **33**: 270–276.
27. Cosset FL, Takeuchi Y, Battini JL, Weiss RA, Collins MK. High-titer packaging cells producing recombinant retroviruses resistant to human serum. *J Virol* 1995; **69**: 7430–7436.
28. Soriano P. Generalized lacZ expression with the ROSA26 Cre reporter strain. *Nat Genet* 1999; **21**: 70–71.
29. Magin TM, McWhir J, Melton DW. A new mouse embryonic stem cell line with good germ line contribution and gene targeting frequency. *Nucleic Acids Res* 1992; **20**: 3795–3796.
30. Kalderon D, Roberts BL, Richardson WD, Smith AE. A short amino acid sequence able to specify nuclear location. *Cell* 1984; **39**: 499–509.
31. Price J, Turner D, Cepko C. Lineage analysis in the vertebrate nervous system by retrovirus-mediated gene transfer. *Proc Natl Acad Sci U S A* 1987; **84**: 156–160.
32. Jooss K, Turka LA, Wilson JM. Blunting of immune responses to adenoviral vectors in mouse liver and lung with CTLA4Ig. *Gene Ther* 1998; **5**: 309–319.
33. Grignani F, Kinsella T, Mencarelli A, *et al*. High-efficiency gene transfer and selection of human hematopoietic progenitor cells with a hybrid EBV/retroviral vector expressing the green fluorescence protein. *Cancer Res* 1998; **58**: 14–19.
34. Ory DS, Neugeboren BA, Mulligan RC. A stable human-derived packaging cell line for production of high titer retrovirus/vesicular stomatitis virus G pseudotypes. *Proc Natl Acad Sci U S A* 1996; **93**: 11 400–11 406.
35. Chen C, Okayama H. High-efficiency transformation of mammalian cells by plasmid DNA. *Mol Cell Biol* 1987; **7**: 2745–2752.
36. Church GM, Gilbert W. Genomic sequencing. *Proc Natl Acad Sci U S A* 1984; **81**: 1991–1995.
37. Kinsella TM, Nolan GP. Episomal vectors rapidly and stably produce high-titer recombinant retrovirus. *Hum Gene Ther* 1996; **7**: 1405–1413.
38. Burns JC, Friedmann T, Driever W, Burrascano M, Yee JK. Vesicular stomatitis virus G glycoprotein pseudotyped retroviral vectors: concentration to very high titer and efficient gene transfer into mammalian and nonmammalian cells. *Proc Natl Acad Sci U S A* 1993; **90**: 8033–8037.
39. Arcasoy SM, Latoche JD, Gondor M, Pitt BR, Pilewski JM. Polycations increase the efficiency of adenovirus-mediated gene transfer to epithelial and endothelial cells in vitro. *Gene Ther* 1997; **4**: 32–38.
40. Gagneten S, Le Y, Miller J, Sauer B. Brief expression of a GFP cre fusion gene in embryonic stem cells allows rapid retrieval of site-specific genomic deletions. *Nucleic Acids Res* 1997; **25**: 3326–3331.
41. Seth P, Rosenfeld M, Higginbotham J, Crystal RG. Mechanism of enhancement of DNA expression consequent to cointernalization of a replication-deficient adenovirus and unmodified plasmid DNA. *J Virol* 1994; **68**: 933–940.
42. Tomko RP, Xu R, Philipson L. HCAR and MCAR: the human and mouse cellular receptors for subgroup C adenoviruses and group B coxsackieviruses. *Proc Natl Acad Sci U S A* 1997; **94**: 3352–3356.

43. Sakai K, Mitani K, Miyazaki J. Efficient regulation of gene expression by adenovirus vector-mediated delivery of the CRE recombinase. *Biochem Biophys Res Commun* 1995; **217**: 393–401.
44. Kanegae Y, Takamori K, Sato Y, Lee G, Nakai M, Saito I. Efficient gene activation system on mammalian cell chromosomes using recombinant adenovirus producing Cre recombinase. *Gene* 1996; **181**: 207–212.
45. Gorski JA, Jones KR. Efficient bicistronic expression of cre in mammalian cells. *Nucleic Acids Res* 1999; **27**: 2059–2061.
46. Kolb AF, Siddell SG. Genomic targeting with an MBP-Cre fusion protein. *Gene* 1996; **183**: 53–60.
47. Kanegae Y, Lee G, Sato Y, *et al.* Efficient gene activation in mammalian cells by using recombinant adenovirus expressing site-specific Cre recombinase. *Nucleic Acids Res* 1995; **23**: 3816–3821.
48. Fernex C, Dubreuil P, Mannoni P, Bagnis C. Cre/loxP-mediated excision of a neomycin resistance expression unit from an integrated retroviral vector increases long terminal repeat-driven transcription in human hematopoietic cells. *J Virol* 1997; **71**: 7533–7540.
49. Roe T, Reynolds TC, Yu G, Brown PO. Integration of murine leukemia virus DNA depends on mitosis. *Embo J* 1993; **12**: 2099–2108.
50. Li Y, Pong RC, Bergelson JM, *et al.* Loss of adenoviral receptor expression in human bladder cancer cells: a potential impact on the efficacy of gene therapy. *Cancer Res* 1999; **59**: 325–330.
51. Asaoka K, Tada M, Sawamura Y, Ikeda J, Abe H. Dependence of efficient adenoviral gene delivery in malignant glioma cells on the expression levels of the Coxsackievirus and adenovirus receptor. *J Neurosurg* 2000; **92**: 1002–1008.
52. Chen L, Pulsipher M, Chen D, *et al.* Selective transgene expression for detection and elimination of contaminating carcinoma cells in hematopoietic stem cell sources. *J Clin Invest* 1996; **98**: 2539–2548.
53. Sanchez ER, Hirst M, Scherrer LC, *et al.* Hormone-free mouse glucocorticoid receptors overexpressed in Chinese hamster ovary cells are localized to the nucleus and are associated with both hsp70 and hsp90. *J Biol Chem* 1990; **265**: 20 123–20 130.
54. Silver DP, Livingston DM. Self-excising retroviral vectors encoding the Cre recombinase overcome Cre-mediated cellular toxicity. *Mol Cell* 2001; **8**: 233–243.